Ferrocene amphiphilic D-π-A dyes: Synthesis, redox behavior and determination of Band Gaps.

Byron López-Mayorga,[1] César I. Sandoval-Chávez[1], Pilar Carreón- Castro[1], Víctor M. Ugalde-Saldívar[2], Fernando Cortés-Guzmán,[3] José G. López-Cortes[3], M. Carmen Ortega-Alfaro*,[1]

[1]*Instituto de Ciencias Nucleares, Universidad Nacional Autónoma de México, Circuito Exterior, Ciudad Universitaria, Coyoacán, Cd. de México, 04510, México.*

[2] *Facultad de Química, Universidad Nacional Autónoma de México, Edificio B. Av. Universidad 3000, Coyoacán, Cd. de México, 04510, México.*

[3]*Instituto de Química, Universidad Nacional Autónoma de México, Circuito Exterior, Cd. Universitaria, Coyoacán, Cd. De México, 04510, México*

Contents

Synthesis of **1a**, **1b** and **3.**

Figure S−1. ^{1}H NMR spectrum of **1a**[Br] in $CDCl_3$ (300 MHz).

Figure S−2. ^{13}C NMR spectrum of **1a**[Br] in $CDCl_3$ (75 MHz).

Figure S-3. ^{1}H NMR spectrum of **1b**[Br] in $CDCl_3$ (300 MHz).

Figure S-4. ^{13}C NMR spectrum of **1b**[Br] in $CDCl_3$ (75 MHz).

Figure S−5. ^{1}H NMR spectrum of **3**[Br] in $CDCl_3$ (300 MHz).

Figure S−6. ^{13}C NMR spectrum of **3**[Br] in $CDCl_3$ (75 MHz).

Figure S-7. ^{1}H NMR spectrum of **2a**[Br] in $CDCl_3$ (300 MHz).

Figure S-8. ^{13}C NMR spectrum of **2a**[Br] in $CDCl_3$ (75 MHz).

Figure S−9. ^{1}H NMR spectrum of **2b**[Br] in $CDCl_3$ (300 MHz).

Figure S−10. ^{13}C NMR spectrum of **2b**[Br] in $CDCl_3$ (75 MHz).

Figure S-11 ^{1}H NMR spectrum of **4**[Br] in $CDCl_3$ (300 MHz).

Figure S-12. ^{13}C NMR spectrum of **4**[Br] in $CDCl_3$ (75 MHz).

Figure S−13. ^{1}H NMR spectrum of **2a**[BF_4] in acetone-d_6 (300 MHz).

Figure S−14. ^{19}F NMR spectrum of **2a**[BF_4] in $CDCl_3$ (282 MHz).

Figure S−15. ^{1}H NMR spectrum of **2b**[BF_4] in acetone-d_6 (300 MHz).

Figure S−16. ^{19}F NMR spectrum of **2b**[BF_4] in $CDCl_3$ (282 MHz).

Figure S−17. ^{1}H NMR spectrum of **4**[BF_4] in $CDCl_3$ (300 MHz).

Figure S−18. ^{19}F NMR spectrum of **4**[BF_4] in $CDCl_3$ (282 MHz).

Synthesis of **6a**, **6b** and **7**.
Figure S−19. ^{1}H NMR spectrum of **6a** in $CDCl_3$ (300 MHz).

Figure S−20. ^{13}C NMR spectrum of **6a** in $CDCl_3$ (75 MHz).

Figure S−21. ^{1}H NMR spectrum of **6b** in $CDCl_3$ (300 MHz).

Figure S−22. ^{13}C NMR spectrum of **6b** in $CDCl_3$ (75 MHz).

Figure S−23. ^{1}H NMR spectrum of **7** in $CDCl_3$ (300 MHz).

Figure S−24. ^{13}C NMR spectrum of **7** in $CDCl_3$ (75 MHz).

Figure S-25. Comparative 1H NMR spectra of (**2a-b**, **4**) [Br] and **6a-b** and **7**

Table S1. Absorption maxima for ferrocenyl amphiphilic D-π-A dyes: Ionic and neutral analogues

Figure S-26. Absorption spectrum in CH_3CN and λ_{onset} of **2a [BF_4]**.

Figure S-27. Absorption spectrum in CH_3CN and λ_{onset} of **2b [BF_4]**.

Figure S-28. Absorption spectrum in CH_3CN and λ_{onset} of **2b [BF_4]**.

Figure S-29. Cyclic voltammograms obtained in 0.1 mol L^{-1} Bu_4NPF_6 acetonitrile solutions on glassy carbon electrode at 100 mVs^{-1}using1mM of **2a[Br].**

Figure S-30. Cyclic voltammograms obtained in 0.1 mol L^{-1} Bu_4NPF_6 acetonitrile solutions on glassy carbon electrode at 100 mVs^{-1}using1 mmol L^{-1} of **2b[Br].**

Figure S-31. Cyclic voltammograms obtained in 0.1 mol L^{-1} Bu_4NPF_6 acetonitrile solutions on glassy carbon electrode at 100 mVs^{-1}using1mmol L^{-1} of **4b**[Br].

Figure S-32. Cyclic voltammograms obtained in 0.1 mol L^{-1} Bu_4NPF_6 acetonitrile solutions on glassy carbon electrode at 100 mVs^{-1}using 1 mmol L^{-1} of **2a[BF_4].**

Figure S-33. Cyclic voltammograms obtained in 0.1 mol L^{-1} Bu_4NPF_6 acetonitrile solutions on glassy carbon electrode at 100 mVs^{-1}using 1 mmol L^{-1} of **2b[BF_4].**

Figure S-34. Cyclic voltammograms obtained in 0.1 mol L^{-1} Bu_4NPF_6 acetonitrile solutions on glassy carbon electrode at 100 mVs^{-1}using1mmol L^{-1} of **4b**[BF_4].

Figure S-35. Comparative cyclic voltammograms obtained in 0.1M Bu_4NPF_6 solutions on glassy carbon electrode at 100 mVs^{-1}using 1 mmol L^{-1} solutions of **TBAB (Tetrabutylammonium bromide) (**teal), **2a**[Br] (red)**2a** [BF_4] (orange).

Figure S-36. Comparative cyclic voltammograms obtained in 0.1 mmol L^{-1} Bu_4NPF_6 solutions on glassy carbon electrode at 100 mVs-1 (negative direction) using 1 mmol L^{-1} solutions of **2a**[Br] (red), **2b**[Br] (green), **4** [Br] (blue) and the corresponding precursors salts **1a, 1b** and **3** (black).

Table S2. Potential values of IIap (assigned to Bromide anion), IVap /IIIcp (assigned to heterocyclic cation).

Figure S-37. Cyclic voltammograms to calculate the potential onset of oxidation and reduction for **2a[Br]**

Figure S-38. Cyclic voltammograms to calculate the potential onset of oxidation and reduction for **2b[Br].**

Figure S-39. Cyclic voltammograms to calculate the potential onset of oxidation and reduction for **4**[Br].

Figure S-40. Cyclic voltammograms to calculate the potential onset of oxidation and reduction for **2a[BF$_4$].**

Figure S-41. Cyclic voltammograms to calculate the potential onset of oxidation and reduction for **2b**[BF$_4$].

Figure S-42. Cyclic voltammograms to calculate the potential onset of oxidation and reduction for **4**[BF$_4$]

Computational Section

Optimized geometries for compounds **2a'**, **2b'** and **4'**

Images of molecular orbitals involved in the excited states of each compound

Synthesis of **1a**, **1b** and **3.**

To a round-bottomed flask equipped with a condenser, 2-picoline (0.001 mol) and 1-bromohexadecane (0.0012 mol) were heated in an oil bath at 110°C for 4 hours. After, cooling; diethyl ether was added and a precipitate appeared. The latter was isolated by filtration and washed with diethyl ether, to give **1a** as a white solid (0.21 g, 66%). ^{1}H NMR (300 MHz, $CDCl_3$): 9.53 (d, 1H, CH-Py, *J* = 6 Hz), 8.39 (t, 1H, CH-Py), 8.0 (d, 1H, CH-Py), 7.93 (t, 1H, CH-Py), 4.80 (t, 2H, $–CH_2-N^+$), 2.93 (s, 3H, CH_3-Py), 1.86 (m, 2H, CH_2-alkyl), 1.38 (m, 2H), 1.17 (br s, 25 H, CH_2-alkyl), 0.80 (s, 3H CH_3). ^{13}C NMR (75MHz, $CDCl_3$). δ 154.2 (C-Py), 146.5 (C-Py), 145.2 (C-Py), 130.4 (C-Py), 126.4 (C-Py), 58.5 ($–CH_2-N^+$), 31.9, 30.8, 29.6, 29.5, 29.3, 29.1, 26.3, 22.6, 20.8 (CH_3-Py), 14.1 (CH_3). MS-DART$^+$, *m/z* (%): 318 (100) (M^+); 319 (26) (M^++1).

A similar procedure was conducted using 4-picoline: (**1b**) White Solid (0.23 g 72 %) ^{1}H NMR (300 MHz, $CDCl_3$): δ 9.23 (d, 2H, Py, *J* = 6 Hz), 7.87 (d, 2H, Py, *J* = 6 Hz), 4.81 (t, 2H, $–CH_2-N^+$), 2.61 (s, 3H, CH_3-Py), 1.96 (m, 2H, CH_2-alkyl) 1.19 (br s, 27 H), 0.81 (t, 3H, CH_3). ^{13}C NMR (75 MHz, $CDCl_3$): δ 158. 8 (C-Py), 144.2 (C-Py), 128.9 (C-Py), 61.3 ($–CH_2-N^+$), 31.9, 31.8 29.7, 29.6, 29.5, 29.4, 29.3, 29.1, 26.1, 22.7 (CH_2-alkyl), 22.2 (CH_3-Py), 14. 1(CH_3). MS-DART$^+$, *m/z* (%): 318 (54) (M^+).

A similar procedure was conducted using 4-quinoline: **(3)** Gray solid, (0.26 g, 77%) ^{1}H NMR (300 MHz, $CDCl_3$): δ 10.22 (d, 1H, C-H quinoline, J = 6 Hz), 8.33 (d, 2H, C-H, quinoline), 8.16 (t, 1H, C-H, quinoline), 8.01 (d, 1H, C-H, quinoline), 5.27 (t, 2H, , $–CH_2-N^+$), 2.97, (s, 3H, CH_3-quinoline), 2.02 (m, 2H, CH_2-alkyl), 1.43 (m, 2H, CH_2-alkyl), 1.17 (br, 27H, CH_2-alkyl), 0.81 (t, 3H, CH_3-alkyl). ^{13}C NMR (75 MHz, $CDCl_3$): δ 157.8 (C-H, quinoline), 149.5 (C-H, quinoline), 137.0 (C, quinoline), 135.3 (C-H, quinoline), 129.9 (C-H, quinoline), 129.4 (C, quinoline), 126.9 (C-H, quinoline), 123.5 (C-H, quinoline), 118.9 (C-H, quinoline), 57.8 ($–CH_2-N^+$), 30.3, 29.6, 29.5, 29.4, 29.3, 29.2, 25.5, (CH_2-alkyl) 22.6 (CH_3-quinoline), 14.1 (CH_3-alkyl). MS-DART$^+$, *m/z* (%): 369 (25) (M^+ + 1); 368 (80) (M^+); 144(100) (M^+-$C_{16}H_{32}$).

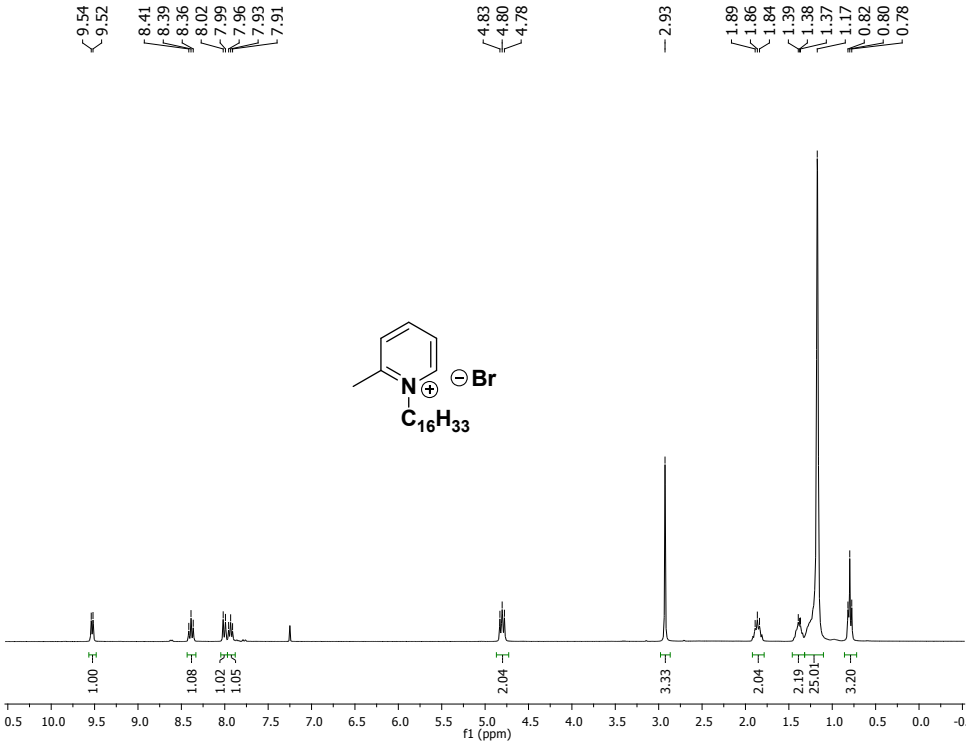

Figure S-1. ^{1}H NMR spectrum of **1a** in $CDCl_3$ (300 MHz).

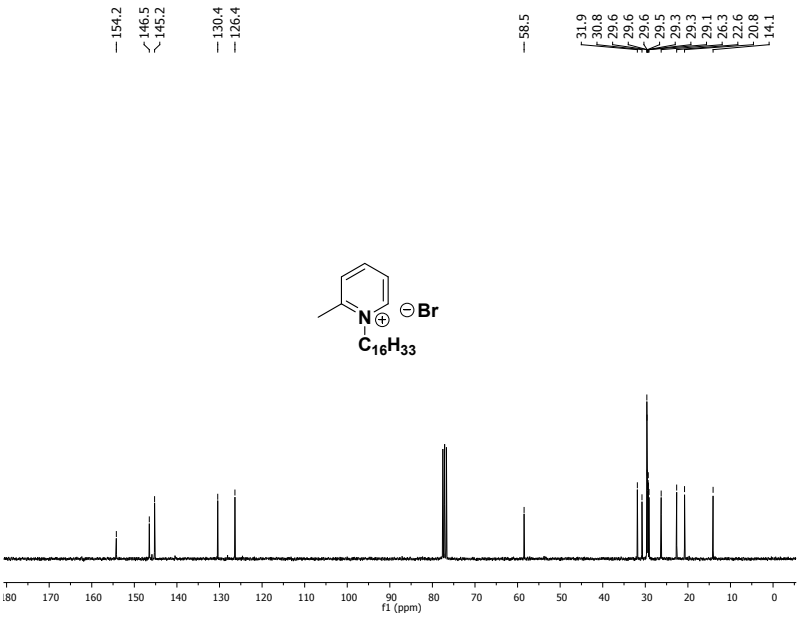

Figure S−2. ^{13}C NMR spectrum of **1a** in $CDCl_3$ (75 MHz).

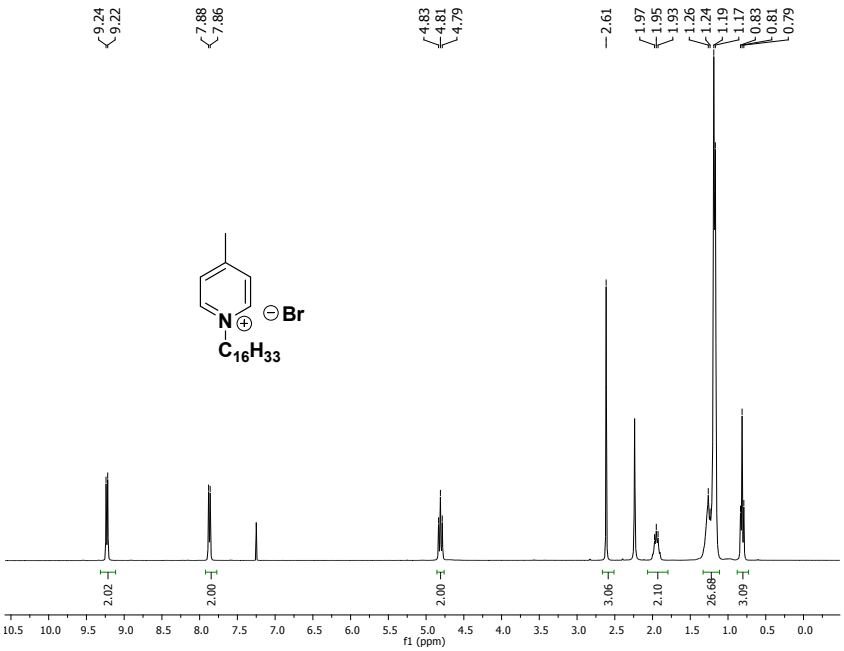

Figure S−3. ^{1}H NMR spectrum of **1b** in $CDCl_3$ (300 MHz).

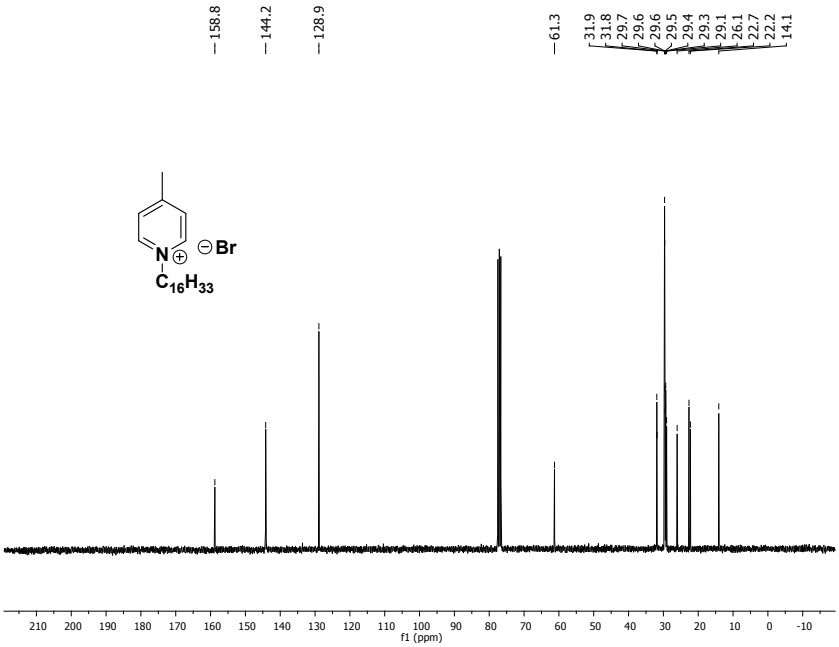

Figure S−4. ^{13}C NMR spectrum of **1b** in $CDCl_3$ (75 MHz).

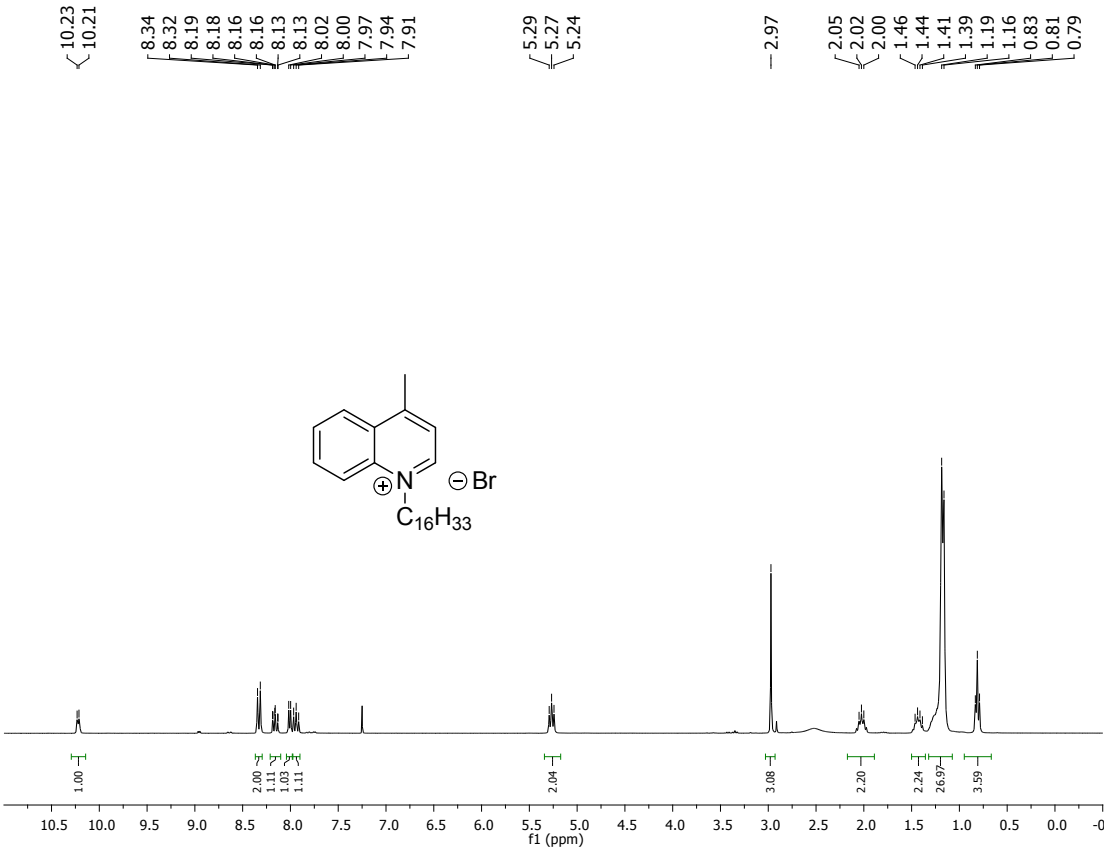

Figure S−5. ^{1}H NMR spectrum of **3** in $CDCl_3$ (300 MHz).

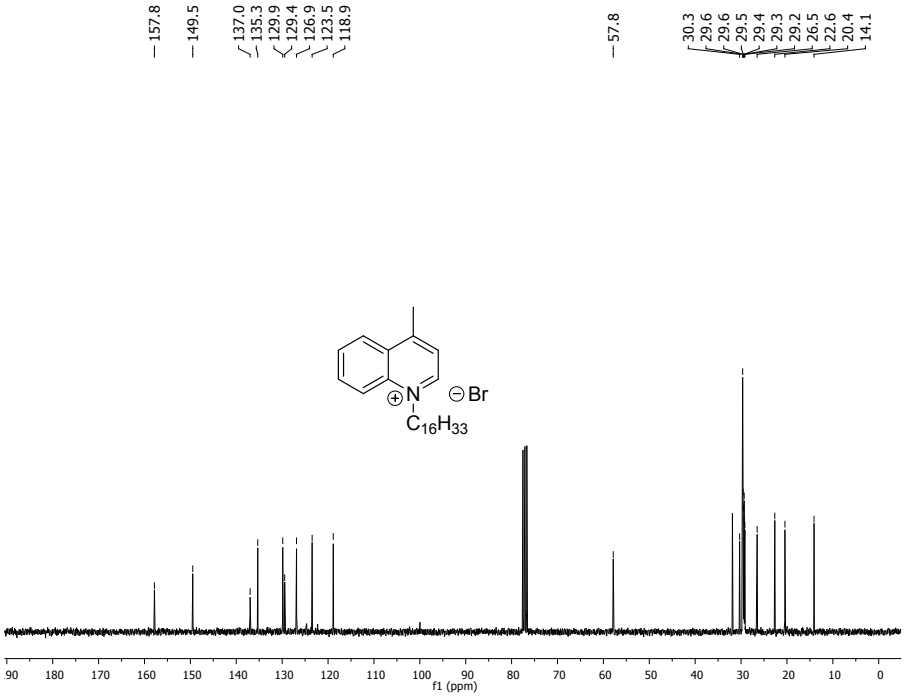

Figure S−6. ^{13}C NMR spectrum of **3**. in $CDCl_3$ (75MHz).

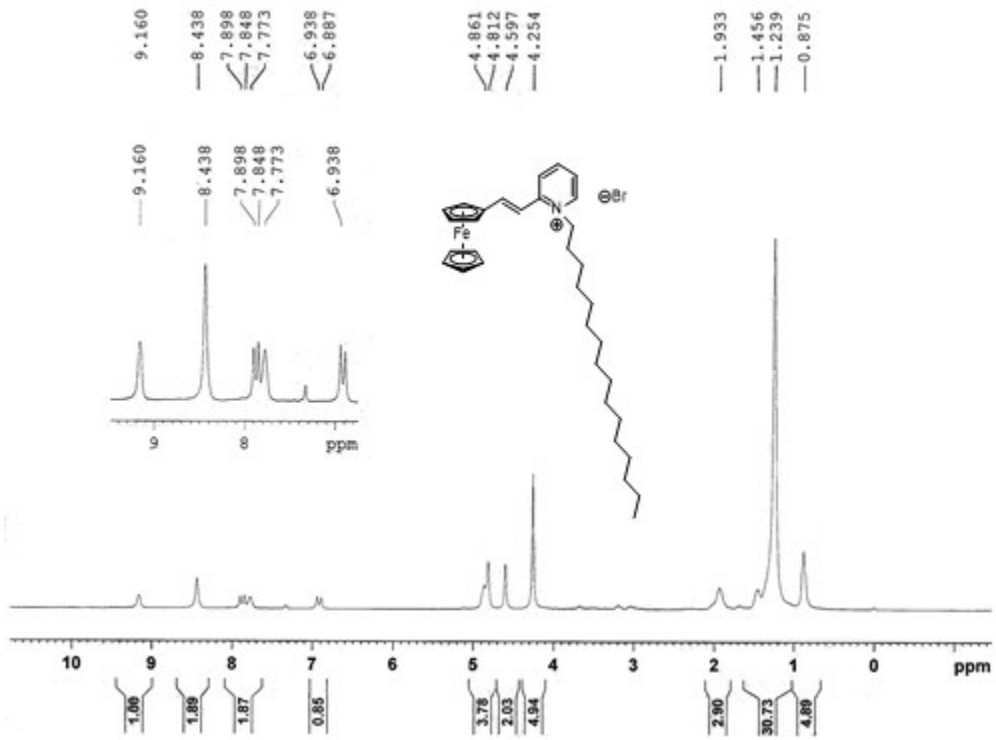

Figure S−7. ^{1}H NMR spectrum of **2a**[Br] in $CDCl_3$ (300MHz).

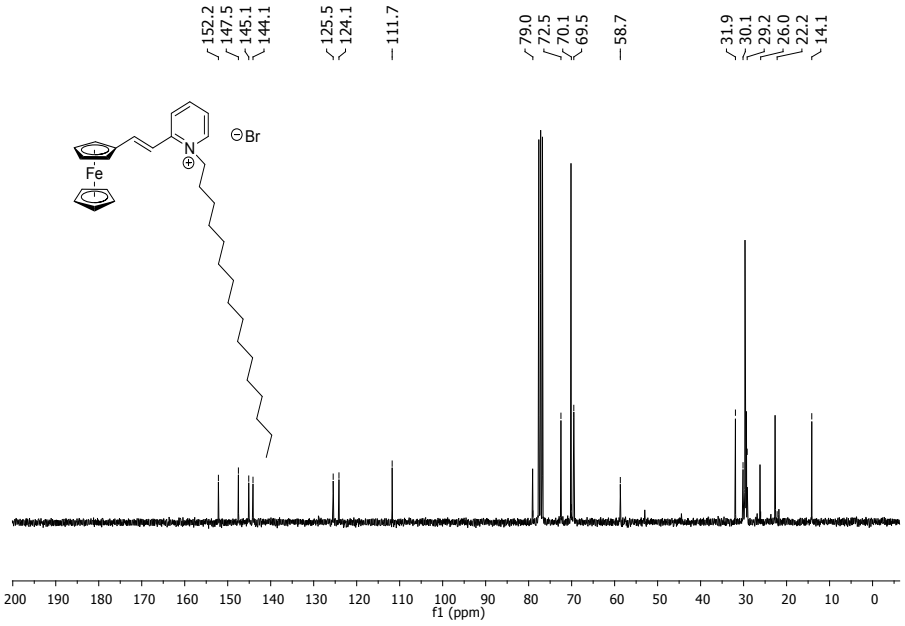

Figure S−8. ^{13}C NMR spectrum of **2a**[Br] in $CDCl_3$ (75MHz).

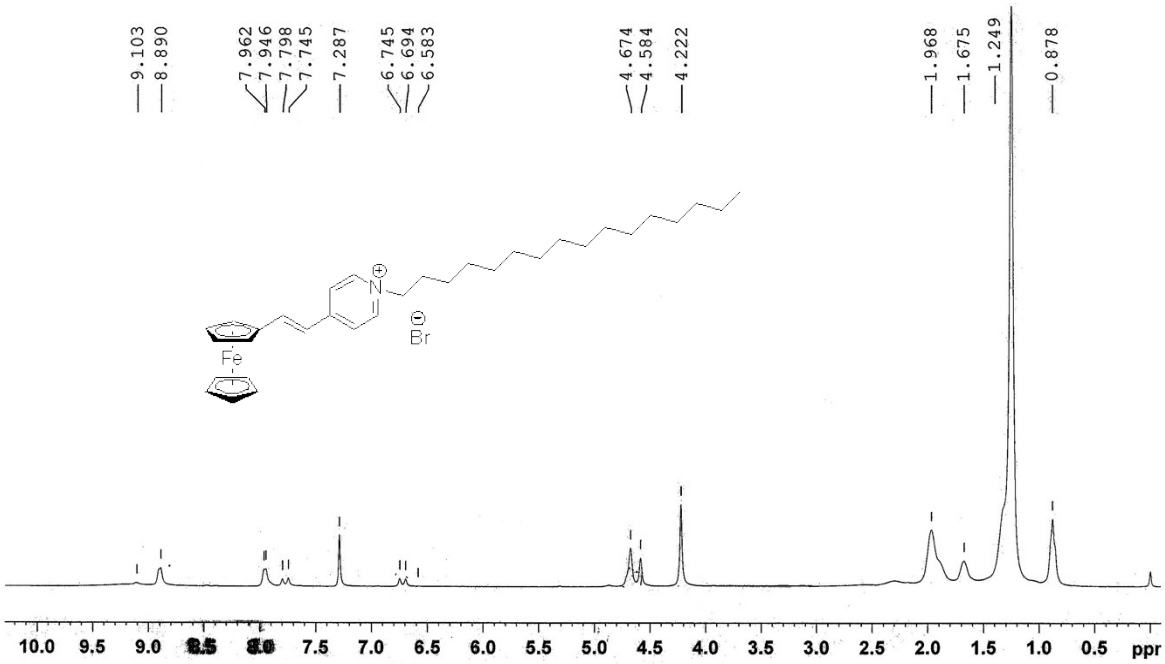

Figure S−9. ^{1}H NMR spectrum of **2b**[Br] in $CDCl_3$ (300MHz).

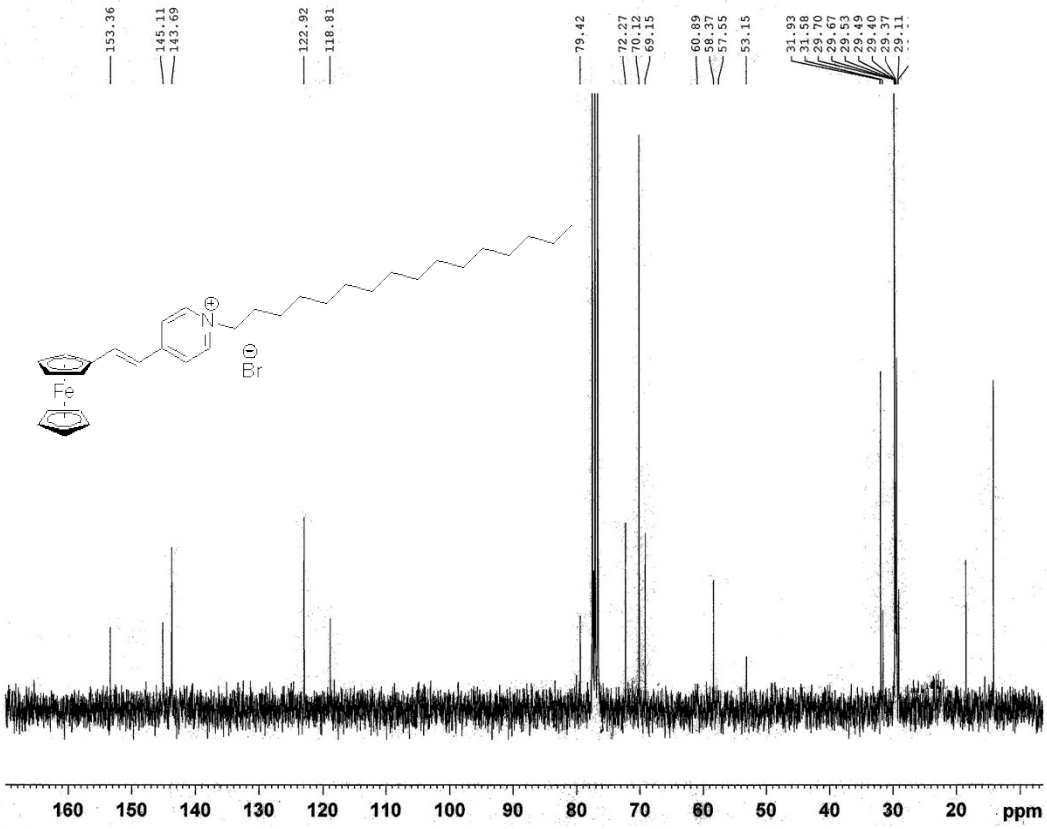

Figure S−10. ^{13}C NMR spectrum of **2b**[Br] in $CDCl_3$ (75MHz).

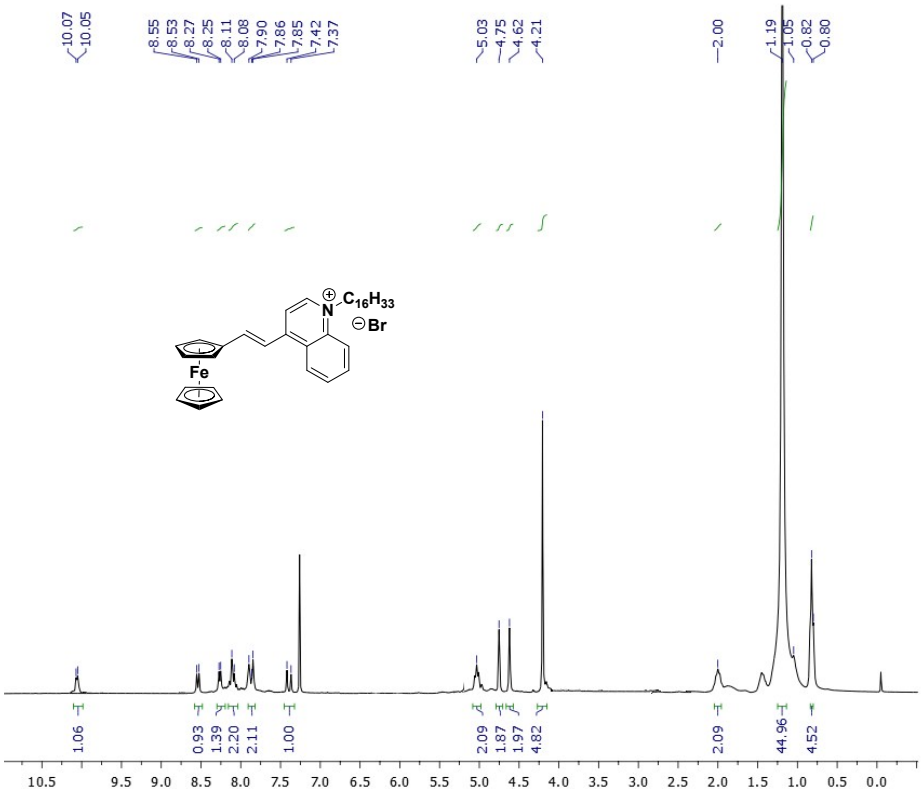

Figure S−11. ^{1}H NMR spectrum of **4**[Br]. in $CDCl_3$ (300MHz).

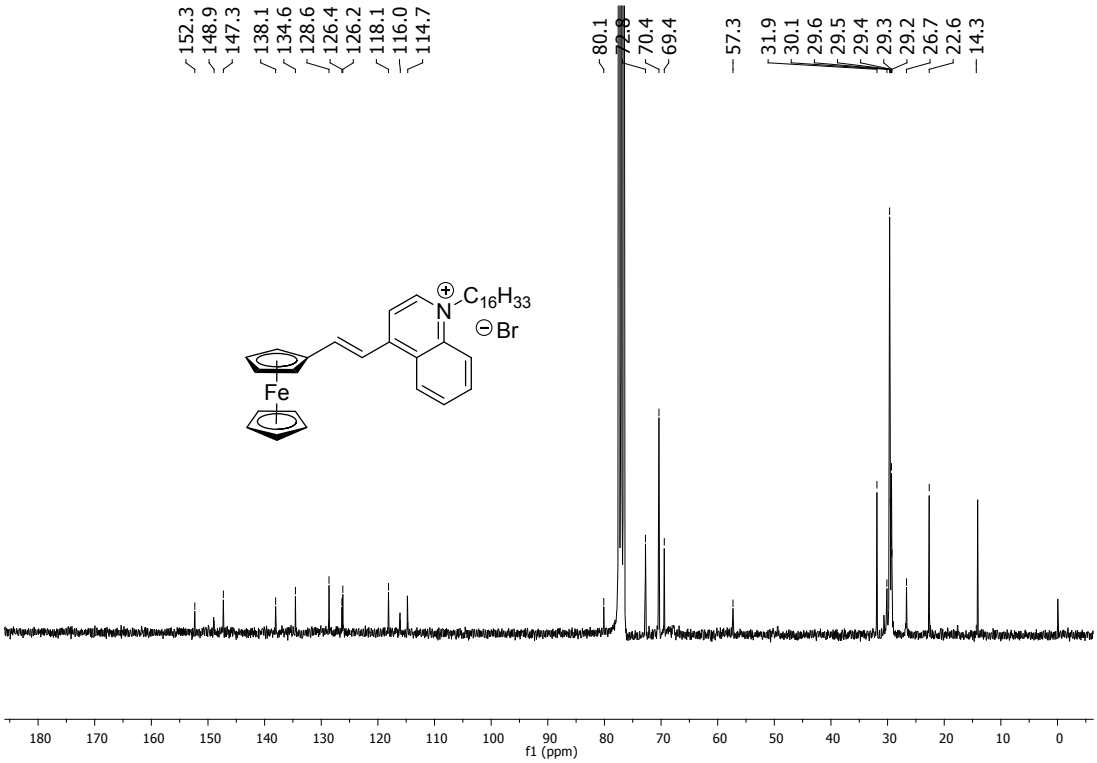

Figure S−12. ^{13}C NMR spectrum of **4**[Br] in $CDCl_3$ (75MHz).

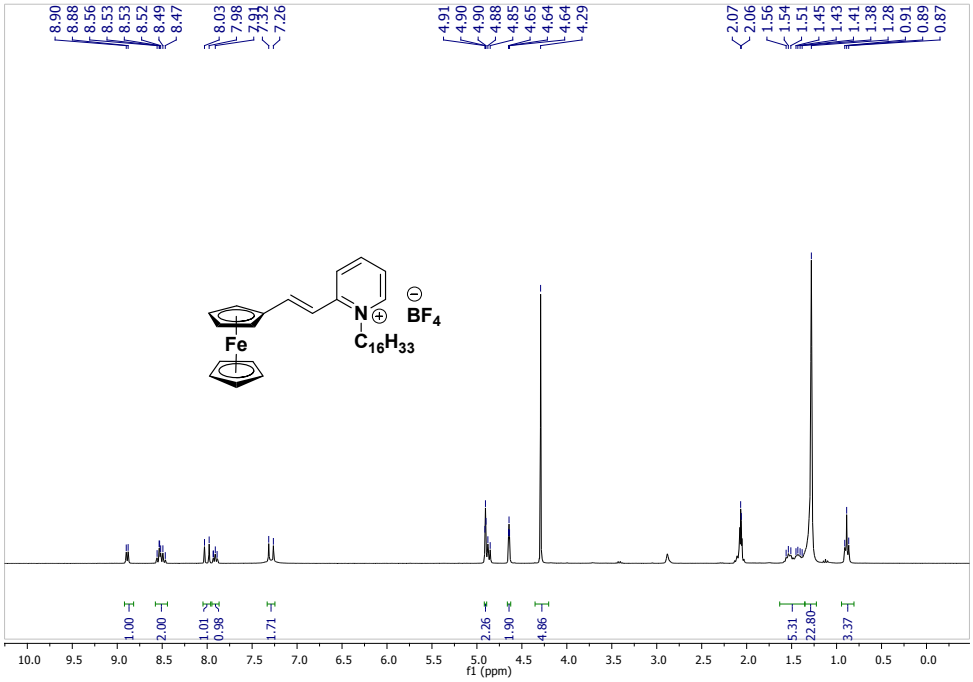

Figure S−13. ^{1}H NMR spectrum of **2a[BF$_4$]** in acetone-d_6 (300 MHz).

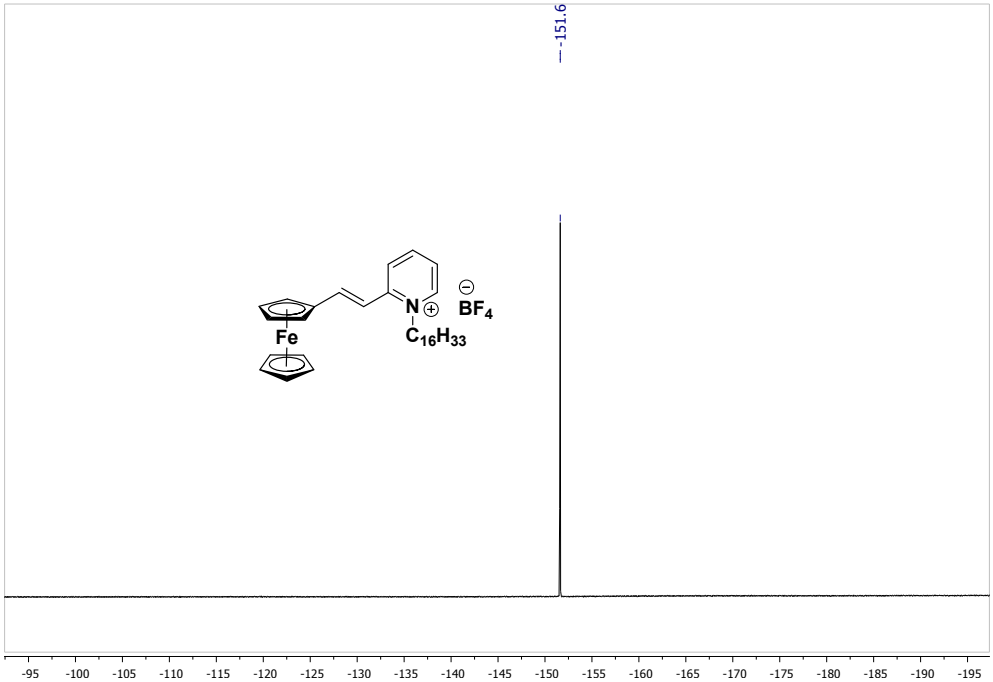

Figure S−14. ^{19}F NMR spectrum of **2a**[BF$_4$] in acetone-d_6 (282 MHz).

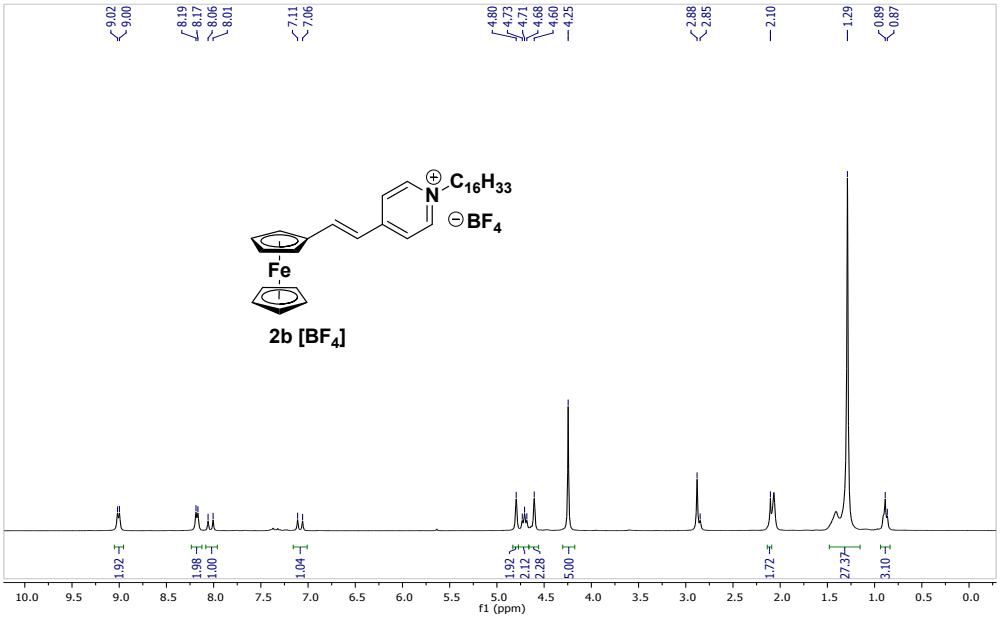

Figure S−15. ^{1}H NMR spectrum of **2b[BF$_4$]** in acetone-d_6 (300 MHz).

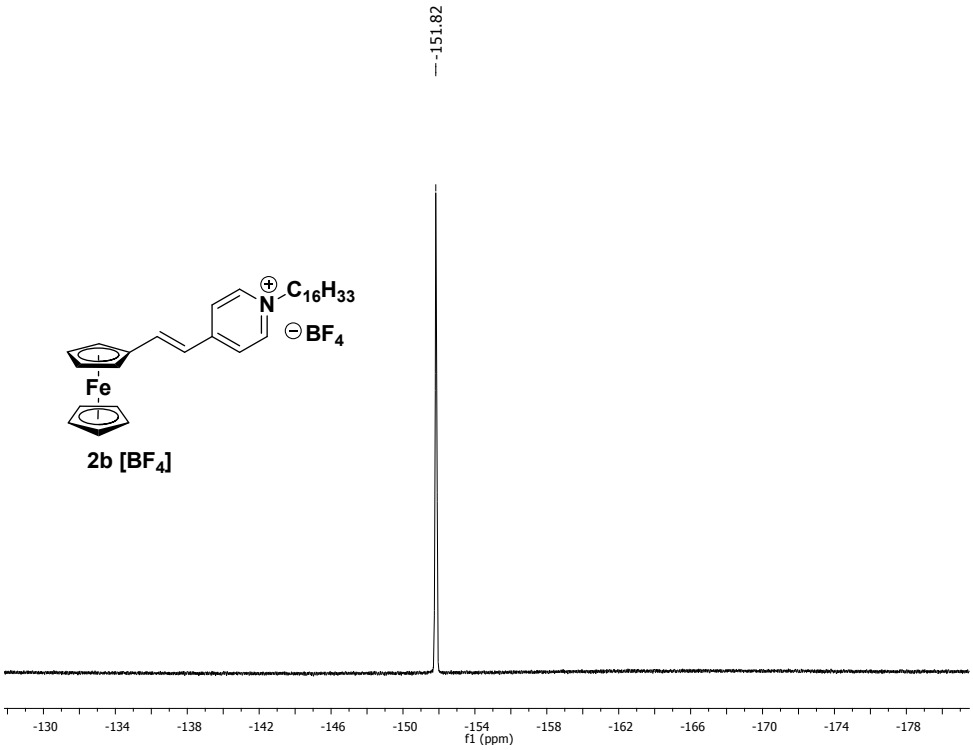

Figure S−16. ^{19}F NMR spectrum of **2b**[BF$_4$] in CDCl$_3$ (282 MHz).

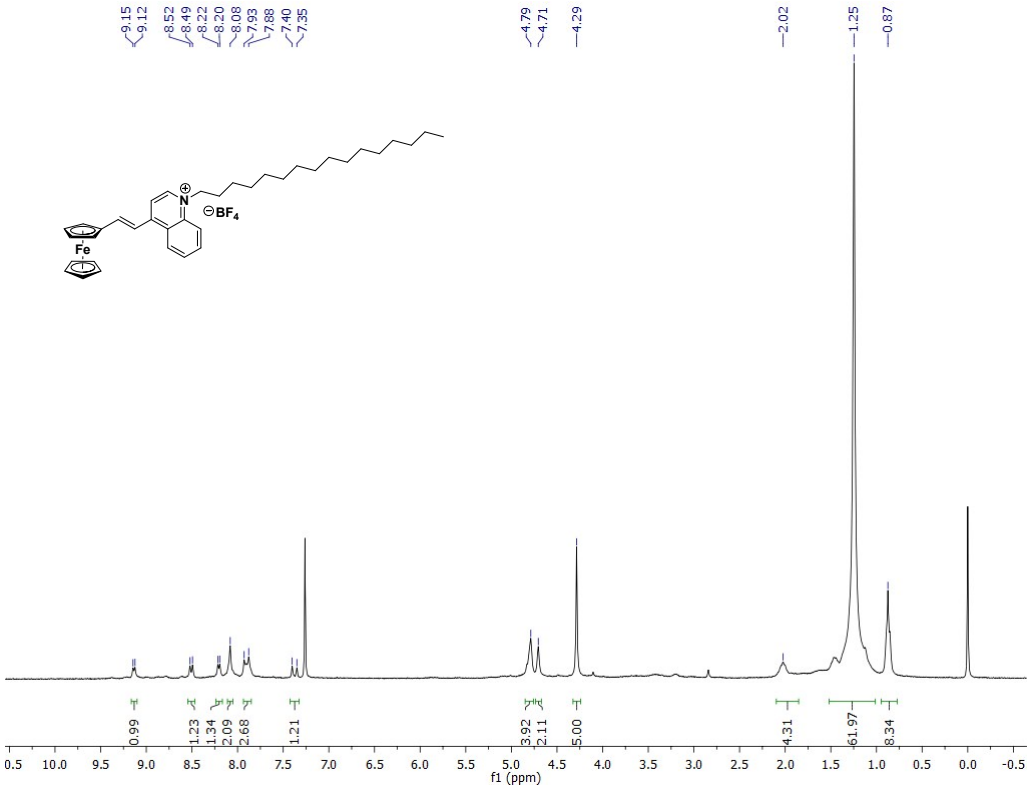

Figure S−17. ^{1}H NMR spectrum of **4[BF$_4$]** in $CDCl_3$ (300MHz).

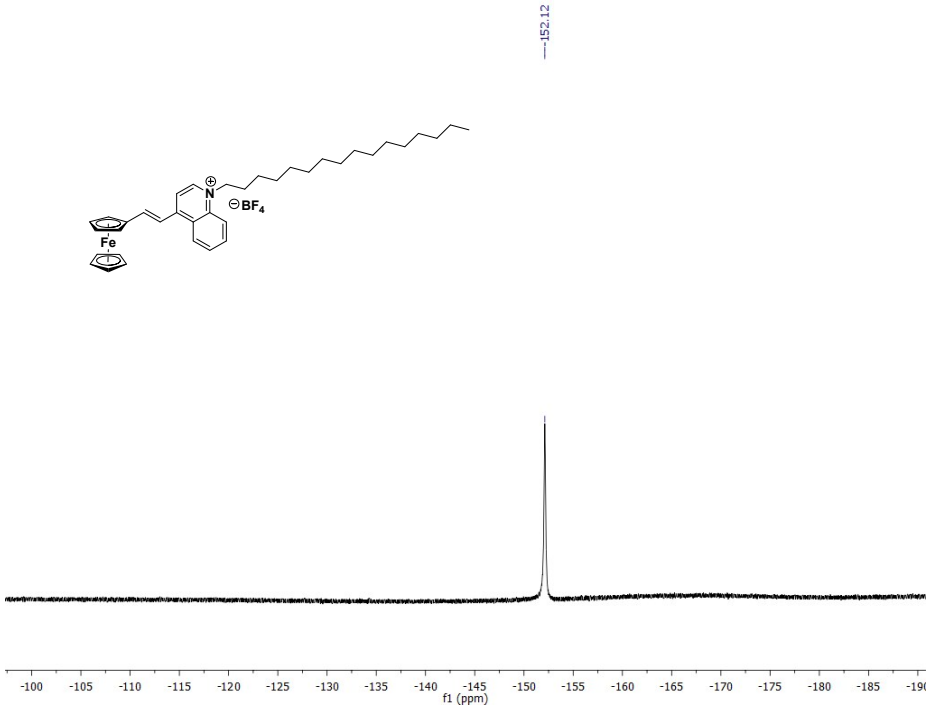

Figure S−18. ^{19}F NMR spectrum of **4[BF$_4$]** in $CDCl_3$ (282 MHz).

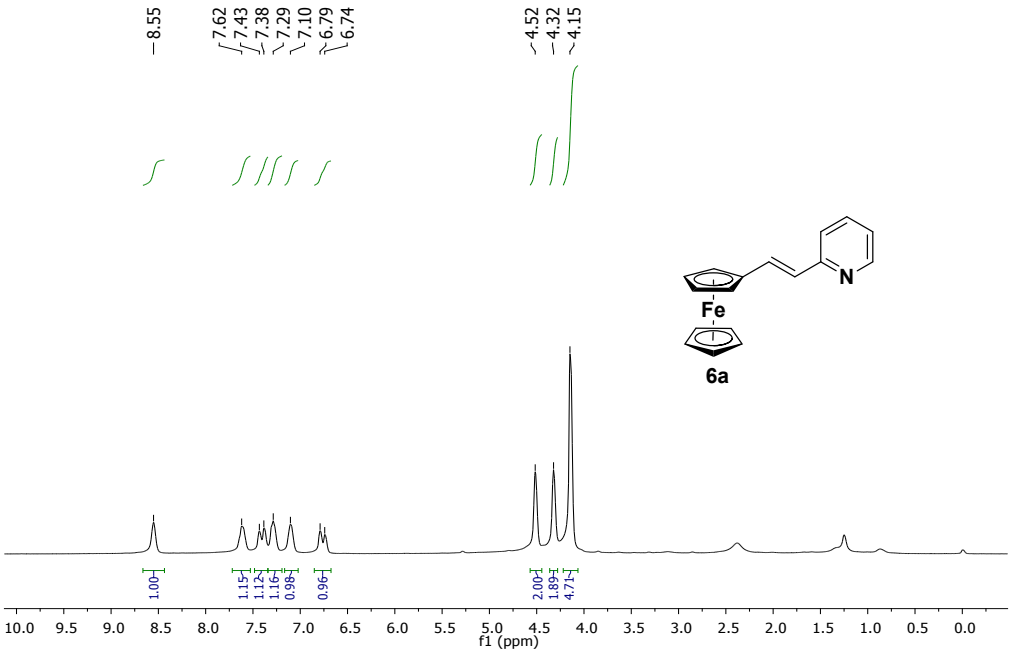

Figure S−19. ^{1}H NMR spectrum of **6a** in $CDCl_3$ (300 MHz).

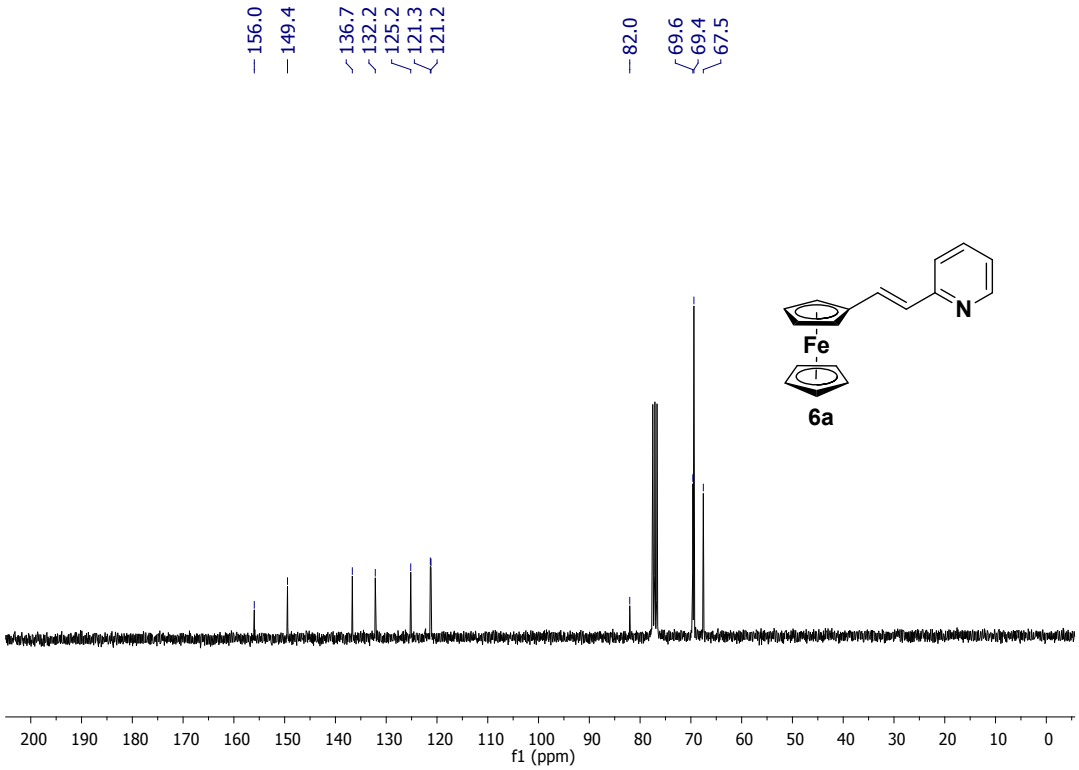

Figure S−20. ^{13}C NMR spectrum of **6a**. in $CDCl_3$ (75MHz).

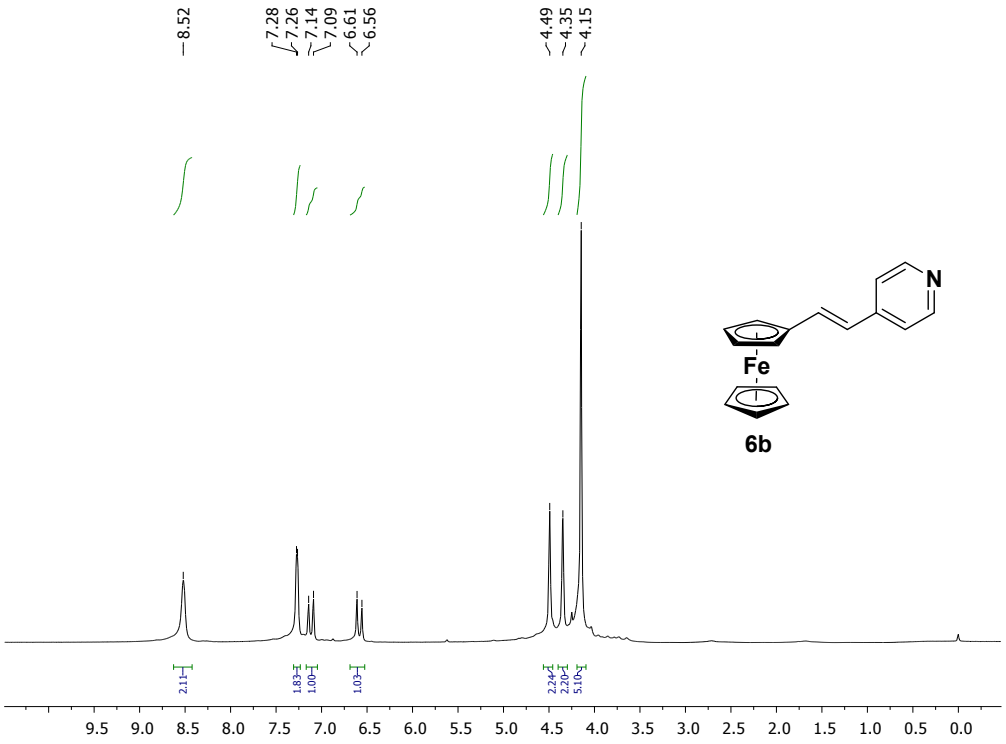

Figure S−21. ^{1}H NMR spectrum of **6b** in $CDCl_3$ (300 MHz).

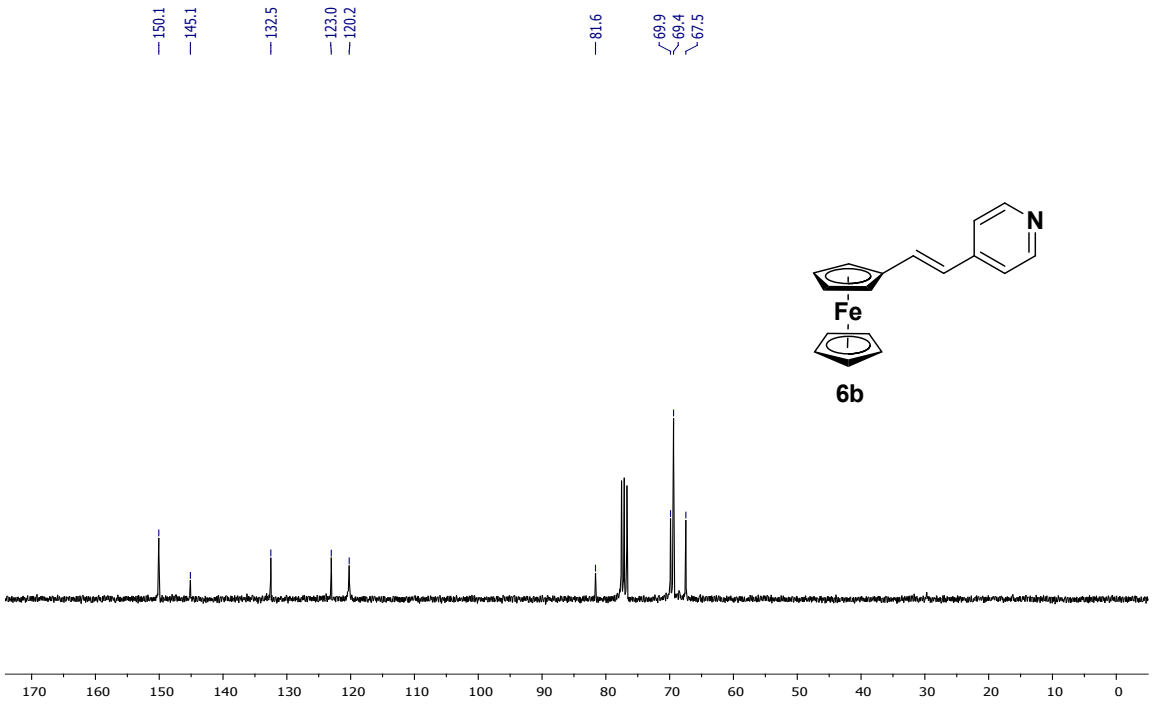

Figure S−22. ^{13}C NMR spectrum of **6b** in $CDCl_3$ (75 MHz).

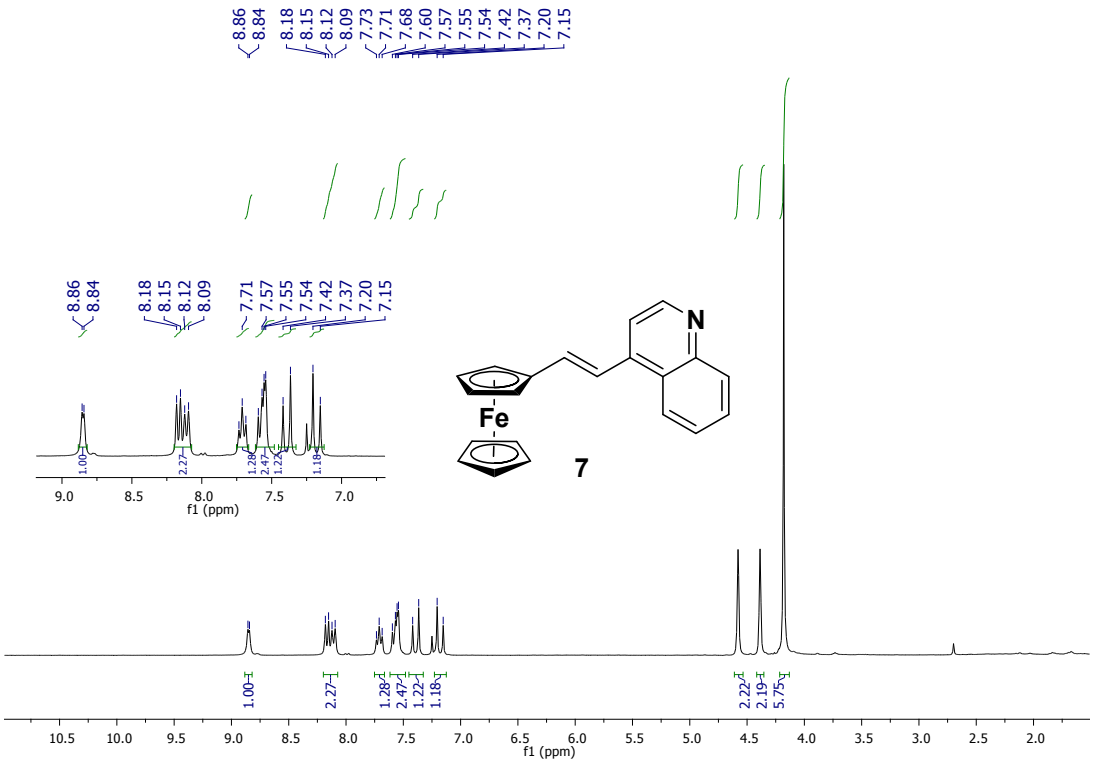

Figure S−23. ^{1}H NMR spectrum of **7** in $CDCl_3$ (300MHz).

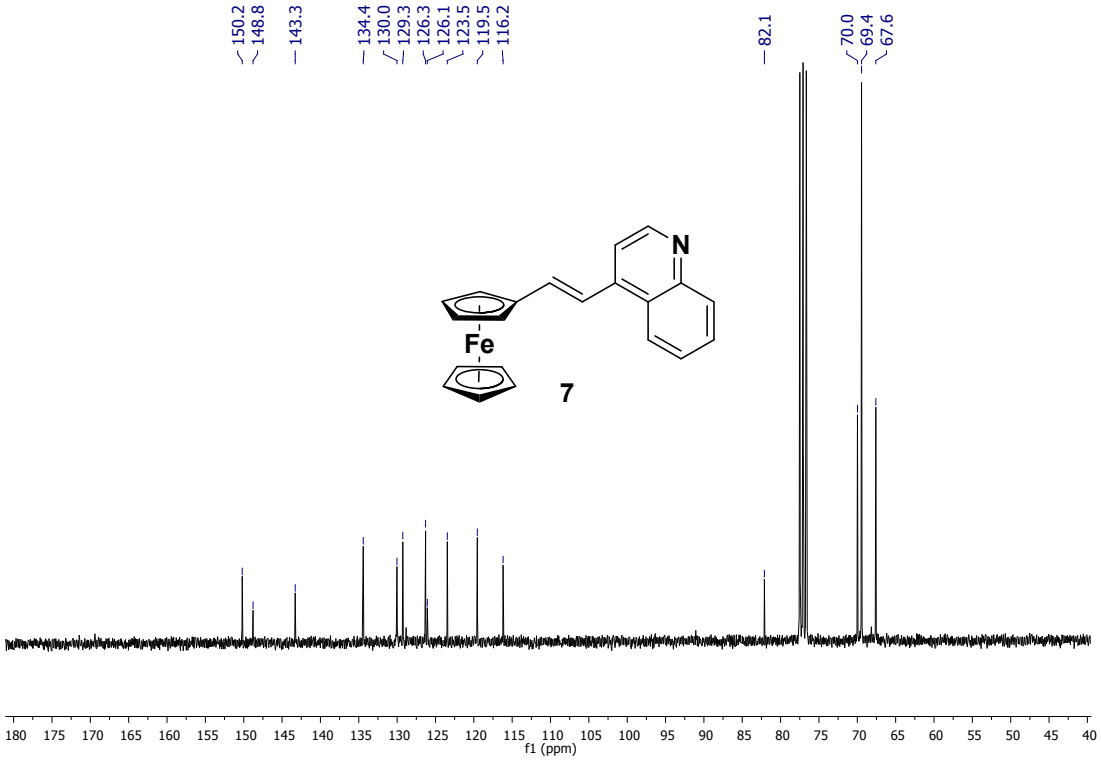

Figure S−24. ^{13}C NMR spectrum of **7** in $CDCl_3$ (75MHz).

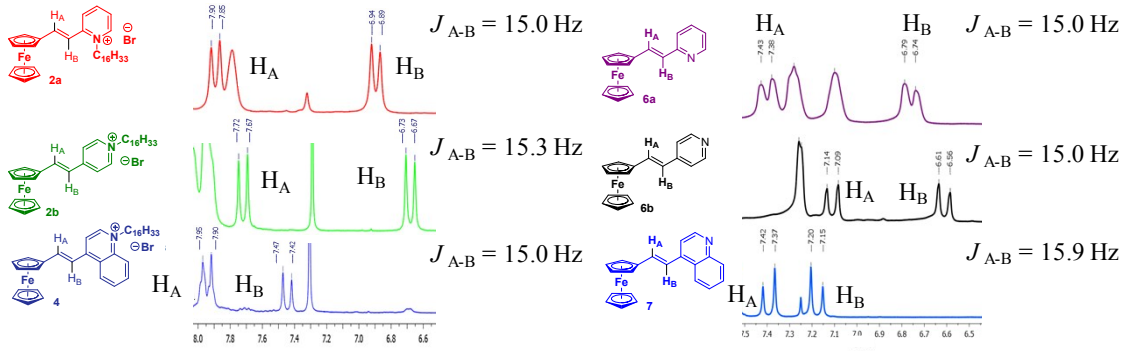

Figure S-25. Comparative ^{1}H NMR spectra of vinyl hydrogens zone of [**2a-b**, **4**][Br], **6a-b** and **7**.

Table S-1. Absorption maxima for ferrocenyl amphiphilic D-π-A dyes: Ionic and neutral analogues. [a]

Entry	Compound	$CHCl_3$		CH_3CN		ΔE^c
		λ_{max}	$\varepsilon_{max}{}^b$	λ_{max}	$\varepsilon_{max}{}^b$	
1	2a[Br]	551 355	3.8 14.1	533 347	2.0 8.7	0.08 0.08
2	2a[BF_4]	550 354	2.3 8.2	530 347	1.9 7.2	0.08 0.07
3	2b[Br]	575 373	5.6 19.7	552 362	3.6 14.9	0.09 0.10
4	2b[BF_4]	578 374	5.3 19.3	551 362	4.5 19.0	0.10 0.11
5	4[Br]	612 409 320	3.5 7.7 7.5	598 406 320	3.3 8.0 7.2	0.04 0.02 0
6	4[BF_4]	621 413 319	4.1 10.4 9.3	601 405 320	3.3 9.5 7.0	0.07 0.06 0.01
7	6a	464 317	1.4 18.5	461 314	1.4 17.9	0.02 0.04
8	6b	467 313	1.6 18.8	465 311	1.2 16.5	0.01 0.02
9	7	478 335	2.0 13.2	476 335	1.8 12.8	0.01 0

[a] λ_{max} (nm), [b]ε ($10^3 mol^{-1} L\ cm^{-1}$), [c]ΔE (eV): Solvent-induced shift [ε_{max} $CHCl_3$ - ε_{max} CH_3CN].

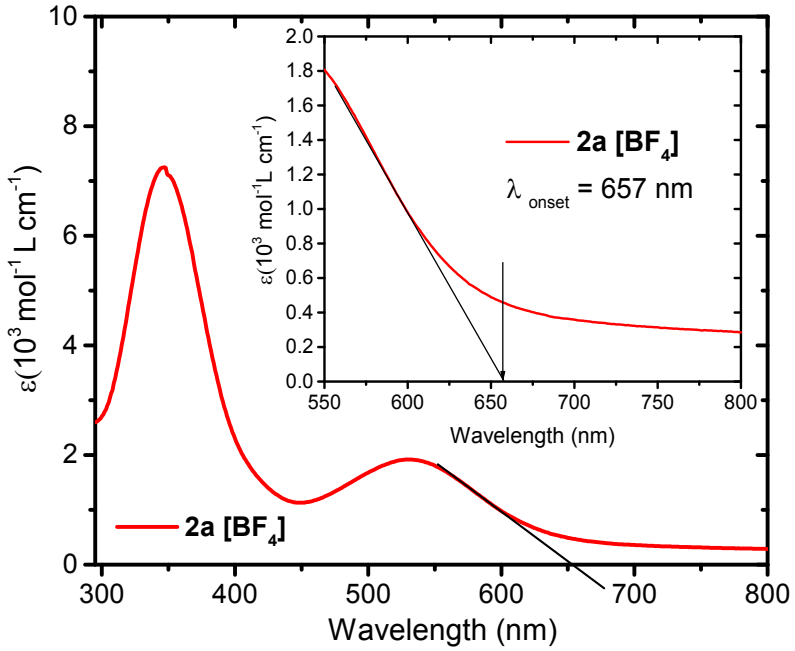

Figure S-26. Absorption spectrum in CH_3CN and λ_{onset} of **2a [BF_4]**.

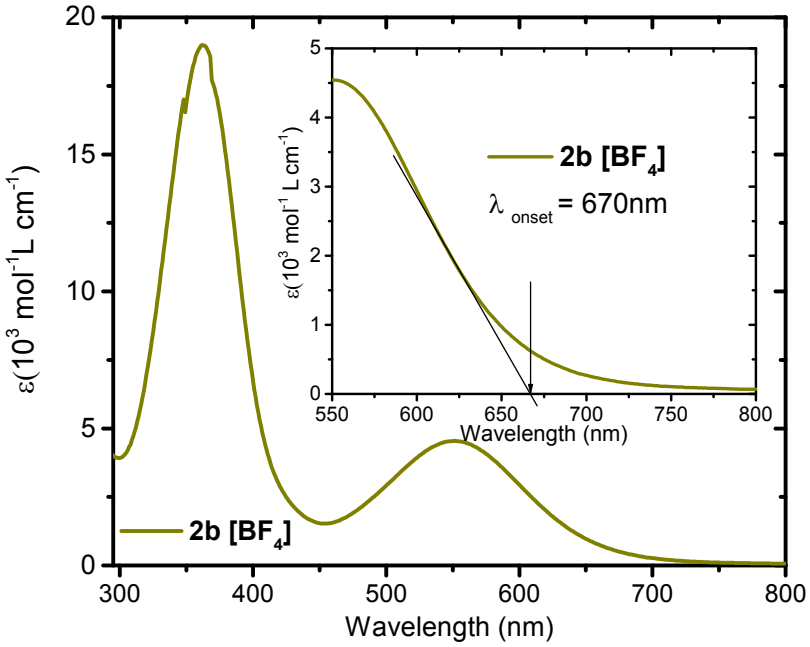

Figure S-27. Absorption spectrum in CH_3CN and λ_{onset} of **2b[BF_4]**.

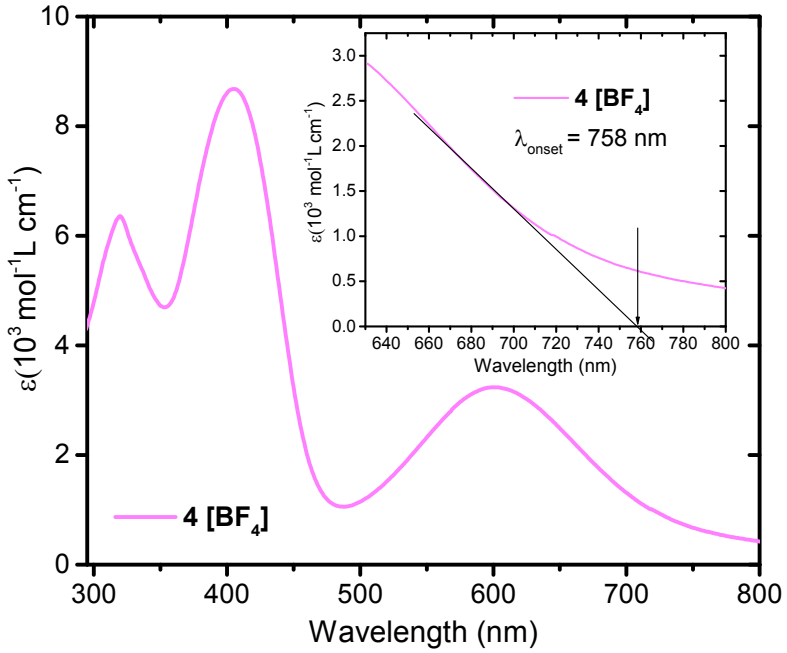

Figure S-28. Absorption spectrum in CH_3CN and λ_{onset} of **4[BF_4]**.

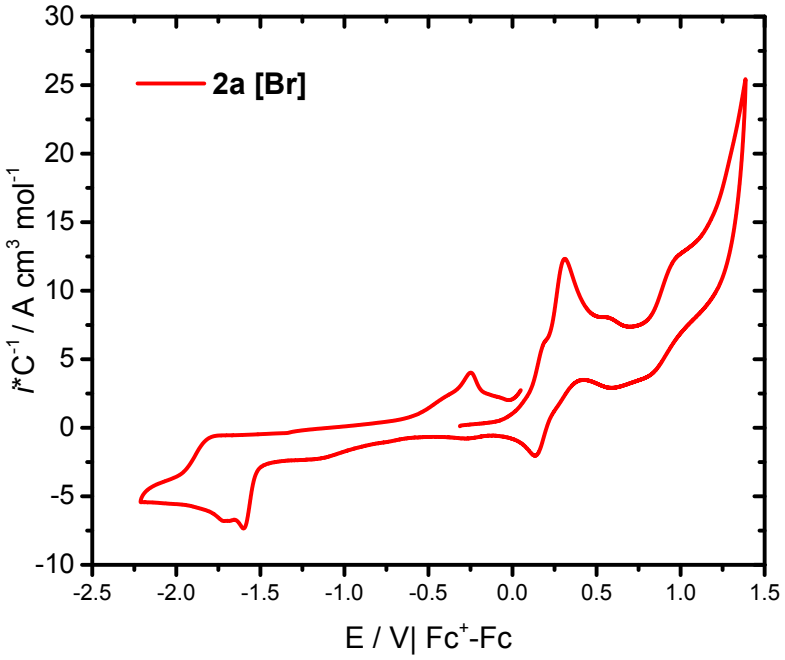

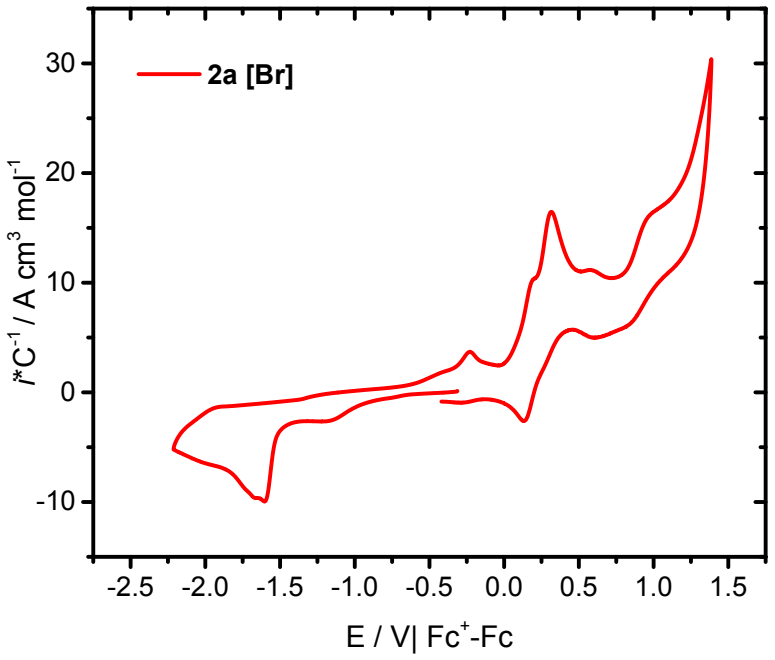

Figure S-29. Cyclic voltammograms obtained in 0.1 mol L^{-1} Bu_4NPF_6 acetonitrile solutions on glassy carbon electrode at 100 mVs^{-1}using 1 mmol L^{-1} of **2a**[Br], started in both positive and negative directions.

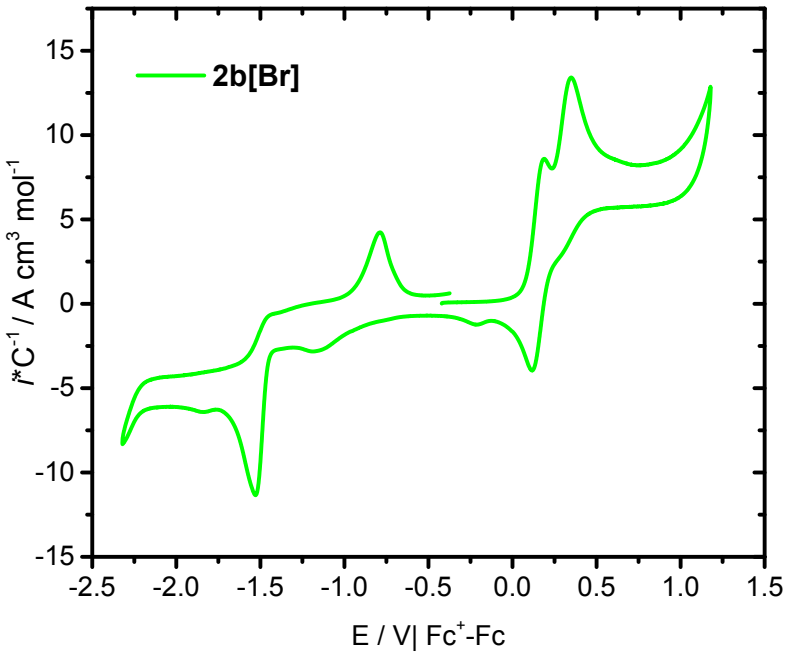

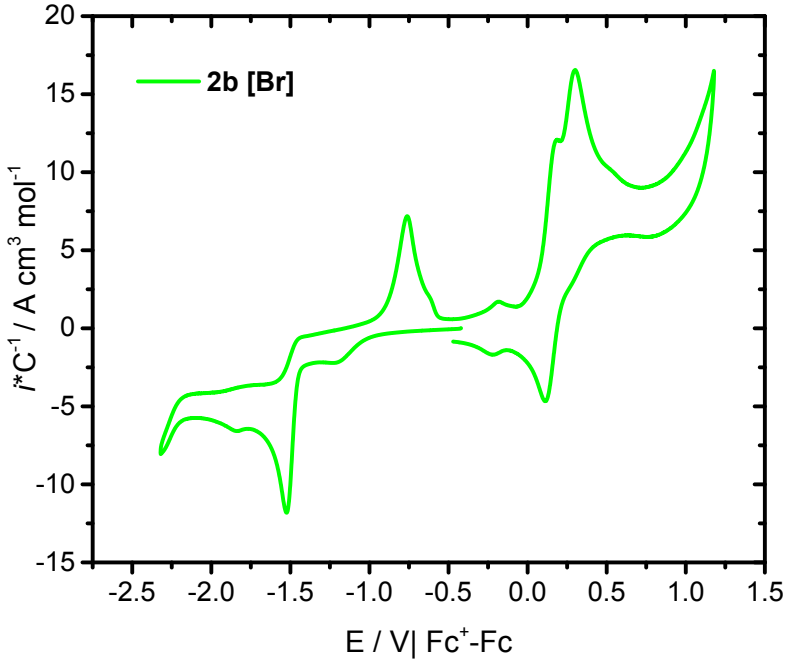

Figure S-30. Cyclic voltammograms obtained in 0.1 mol L^{-1} Bu_4NPF_6 acetonitrile solutions on glassy carbon electrode at 100 mVs^{-1}using1mmol L^{-1} of **2b**[Br], started in both positive and negative directions.

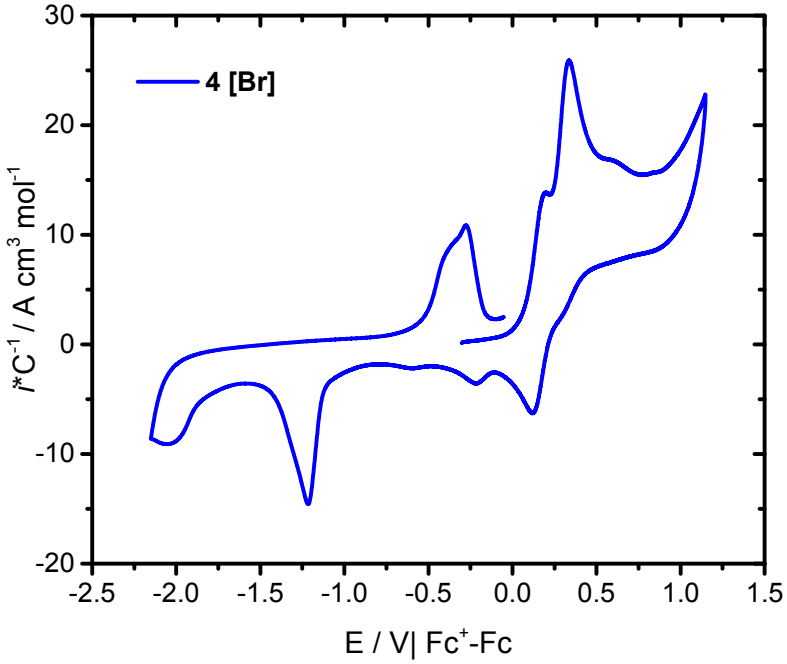

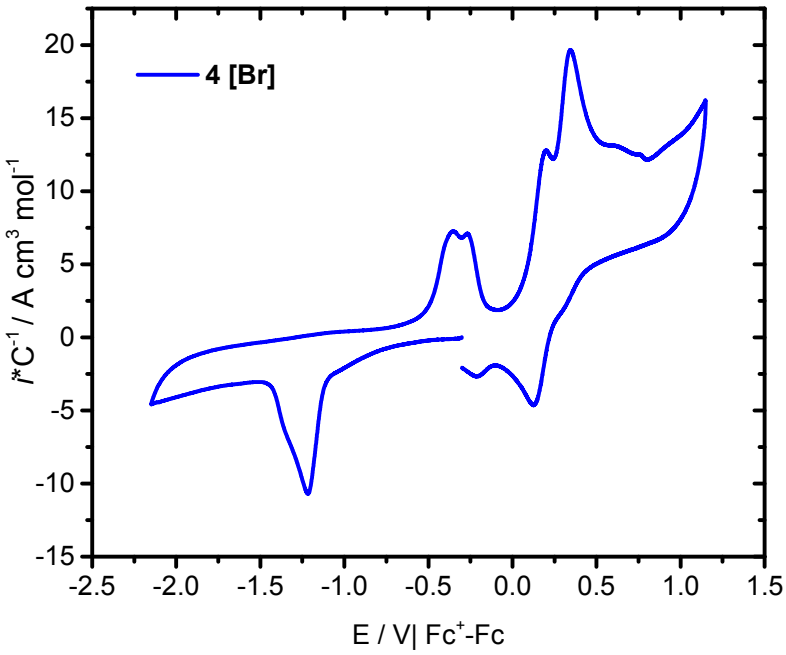

Figure S-31. Cyclic voltammograms obtained in 0.1 mol L^{-1} Bu_4NPF_6 acetonitrile solutions on glassy carbon electrode at 100 mVs^{-1}using1mmol L^{-1} of **4**[Br], started in both positive and negative directions.

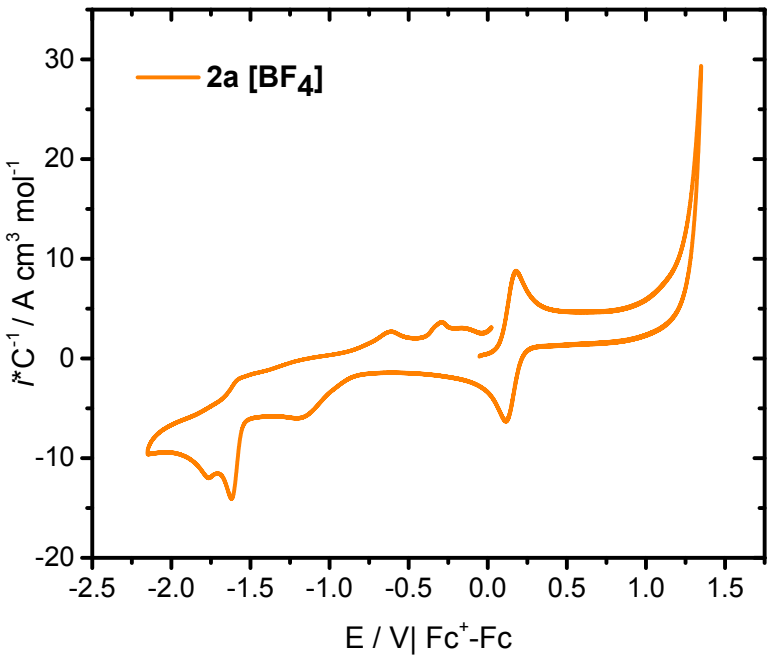

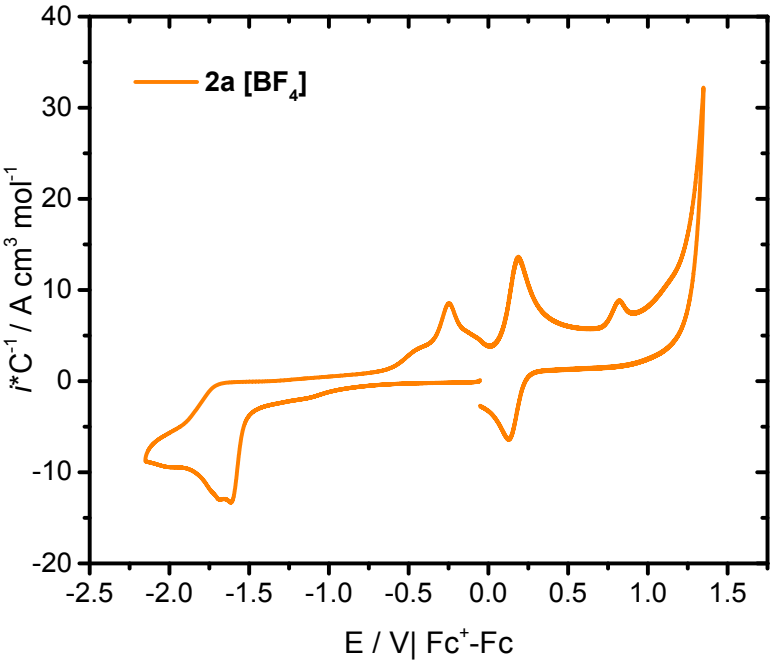

Figure S-32. Cyclic voltammograms obtained in 0.1 mol L^{-1} Bu_4NPF_6 acetonitrile solutions on glassy carbon electrode at 100 mVs^{-1}using 1 mmol L^{-1} of **2a**[BF_4], started in both positive and negative directions.

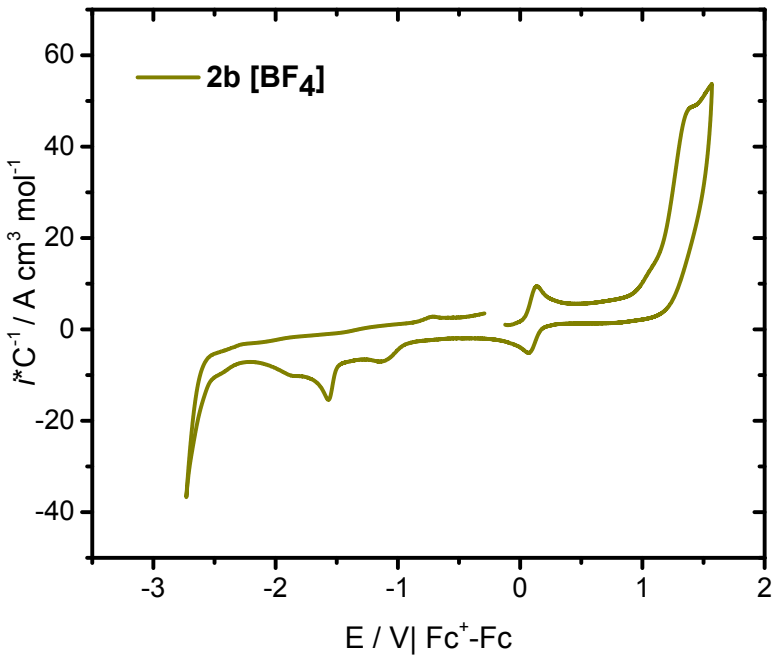

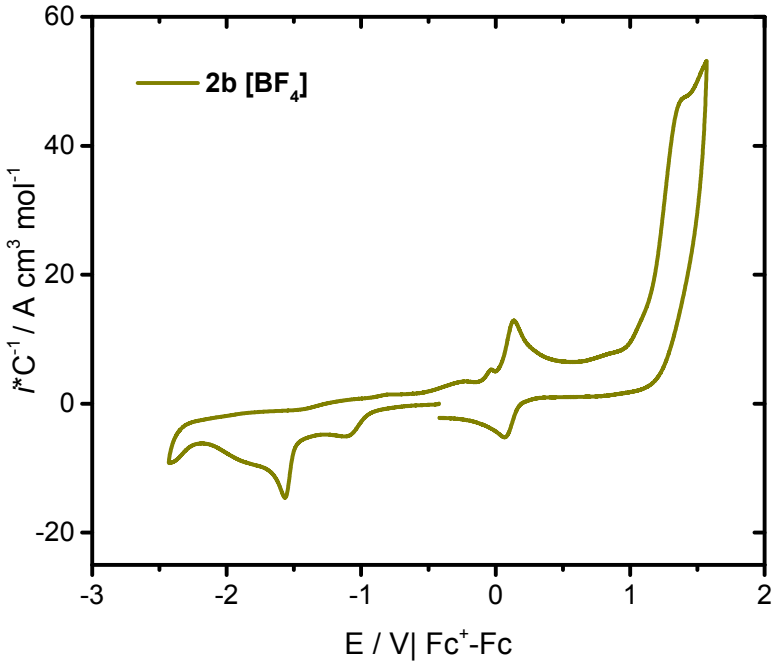

Figure S-33. Cyclic voltammograms obtained in 0.1 mol L^{-1} Bu_4NPF_6 acetonitrile solutions on glassy carbon electrode at 100 mVs^{-1}using1mmol L^{-1} of **2b**[BF_4] , started in both positive and negative directions.

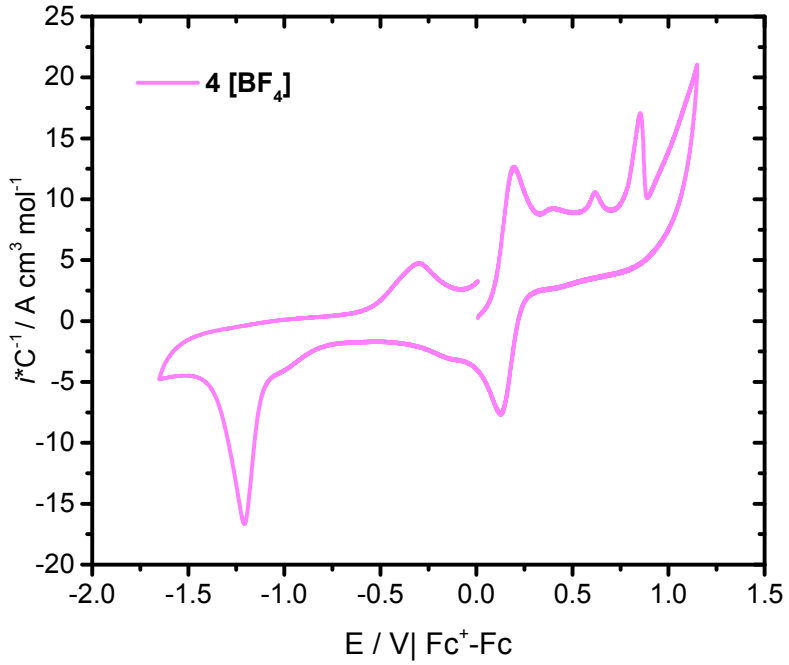

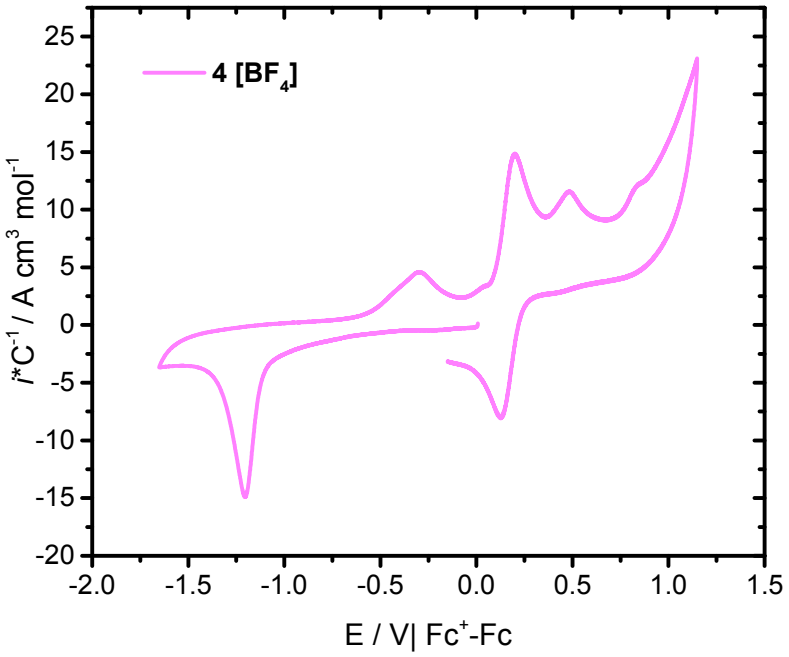

Figure S-34. Cyclic voltammograms obtained in 0.1 mol L^{-1} Bu_4NPF_6 acetonitrile solutions on glassy carbon electrode at 100 mVs^{-1}using1mmol L^{-1} of **4**[BF_4] , started in both positive and negative directions.

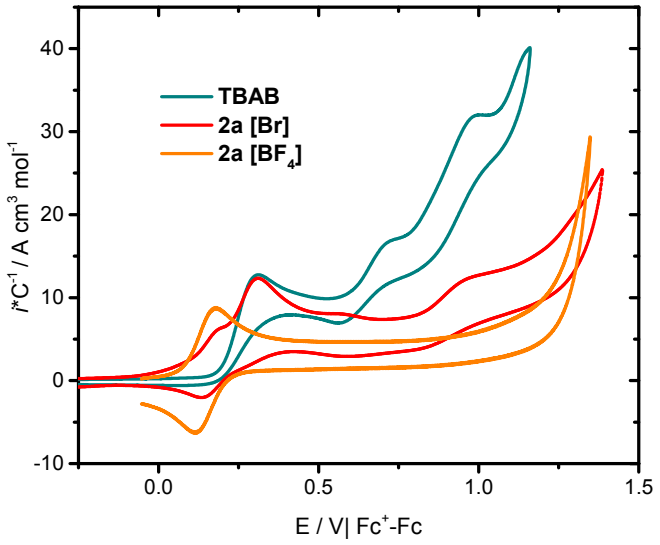

Figure S-35. Comparative cyclic voltammograms obtained in 0.1 mol L^{-1} Bu_4NPF_6 solutions on glassy carbon electrode at 100 mVs^{-1}using 1 mmol L^{-1} solutions of **TBAB (Tetrabutylammonium bromide) (**teal), **2a**[Br] (red)**2a** [BF_4] (orange).

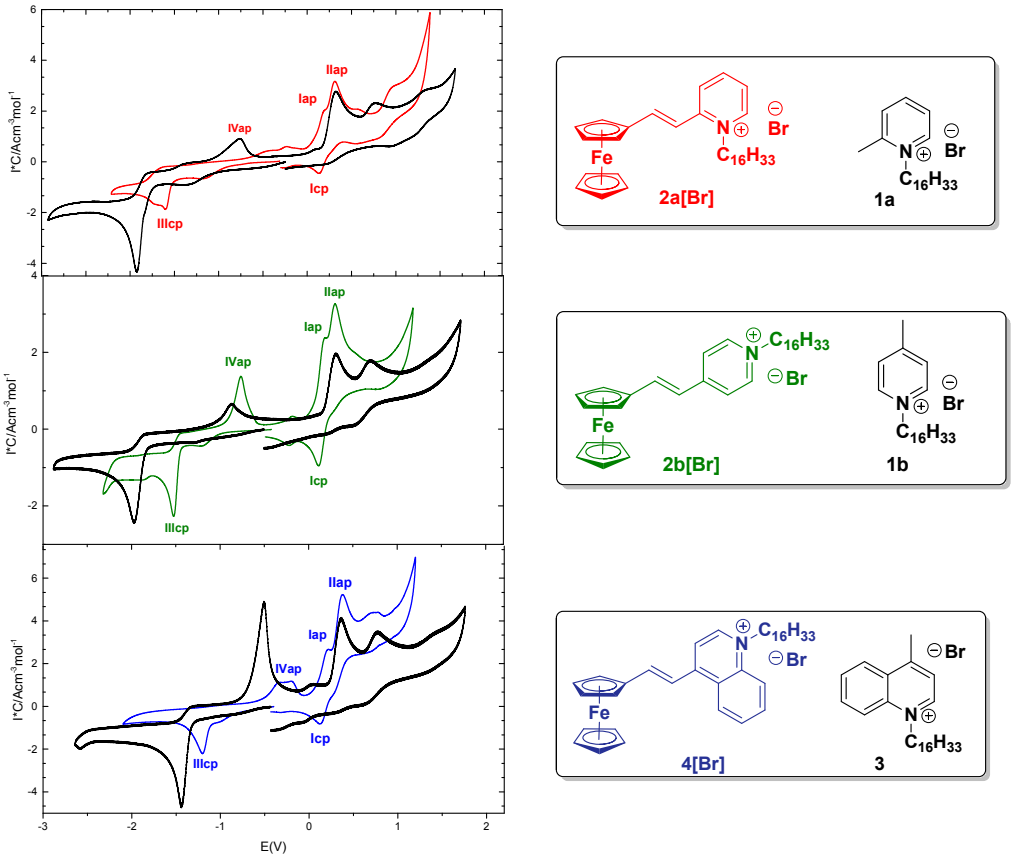

Figure S-36. Comparative cyclic voltammograms obtained in 0.1 mmol L^{-1} Bu_4NPF_6 solutions on glassy carbon electrode at 100 mVs-1 (negative direction) using 1 mmol L^{-1} solutions of **2a**[Br] (red), **2b**[Br] (green), **4** [Br] (blue) and the corresponding precursors salts **1a, 1b** and **3** (black)

Table S2. Potential values of IIap (assigned to Bromide anion), IVap /IIIcp (assigned to heterocyclic cation).

Compound	IIap	IVap	IIIcp
2a[Br]	0.32	-0.50	-1.59
1a	0.33	-0.77	-1.92
2b[Br]	0.29	-0.76	-1.51
1b	0.31	-0.87	-1.97
4[Br]	0.37	-0.34	-1.21
3	0.37	-0.51	-1.42

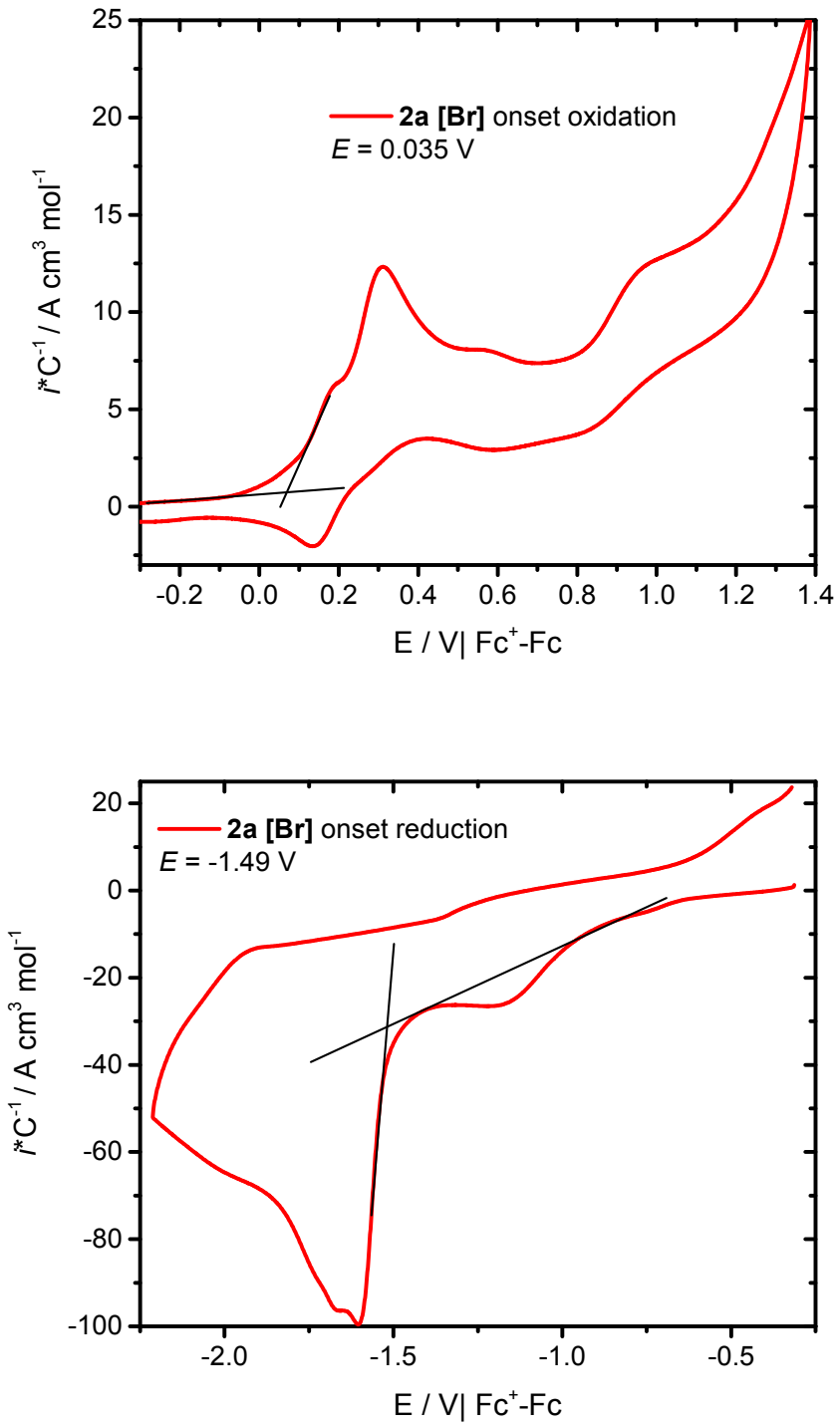

Figure S-37. Cyclic voltammograms to calculate the potential onset of oxidation and reduction for **2a[Br]**

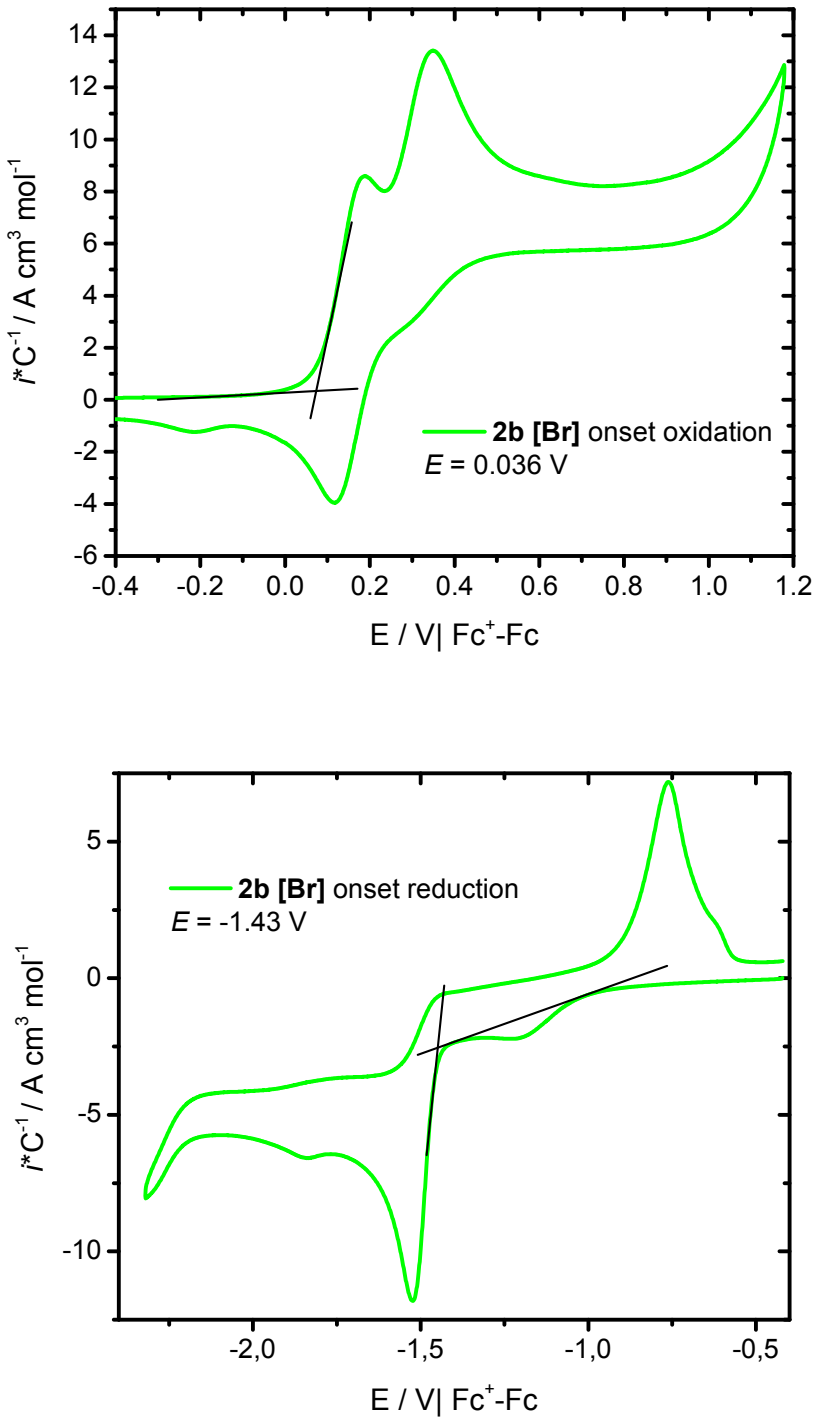

Figure S-38. Cyclic voltammograms to calculate the potential onset of oxidation and reduction for **2b**[Br].

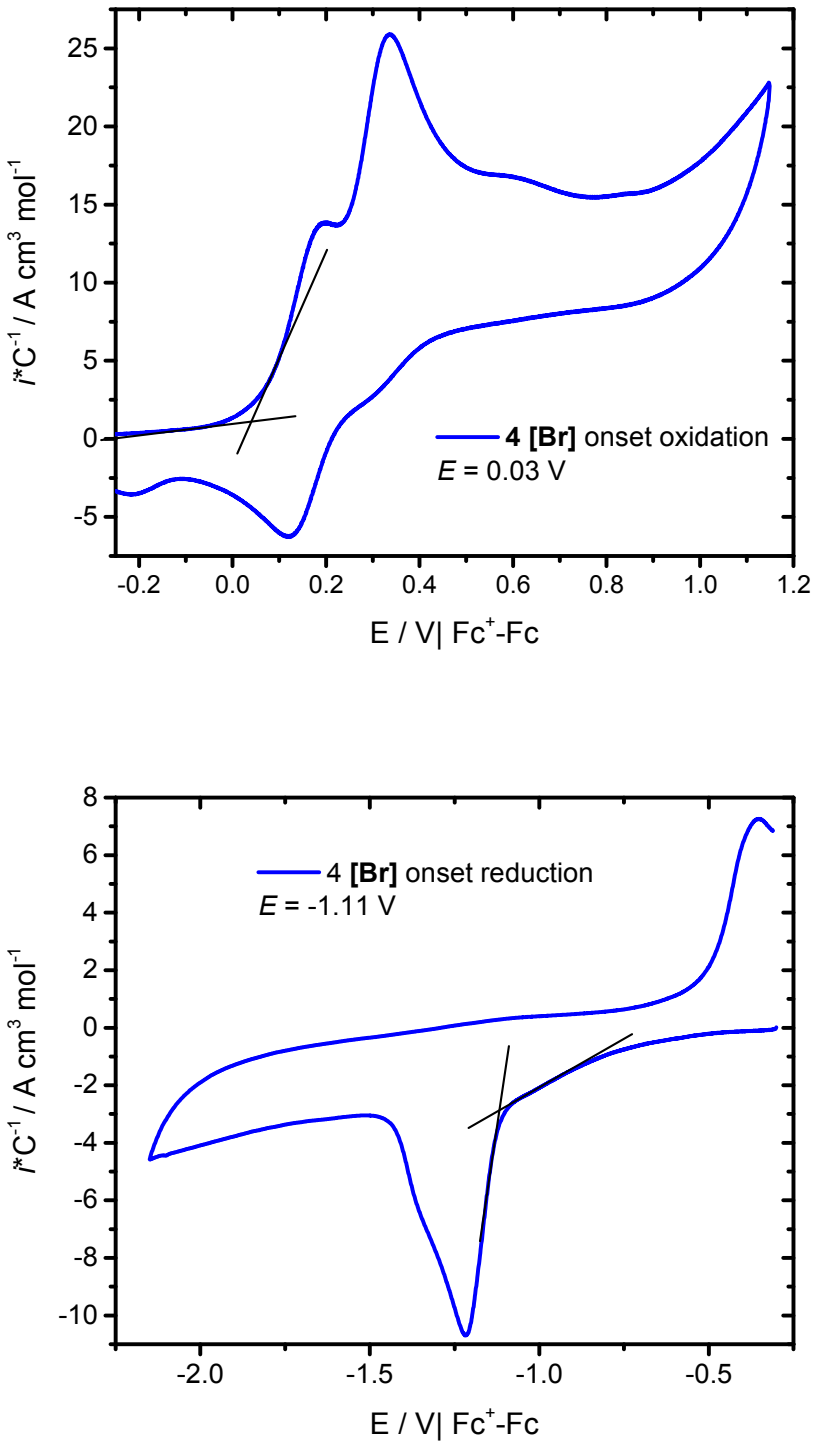

Figure S-39. Cyclic voltammograms to calculate the potential onset of oxidation and reduction for **4**[Br].

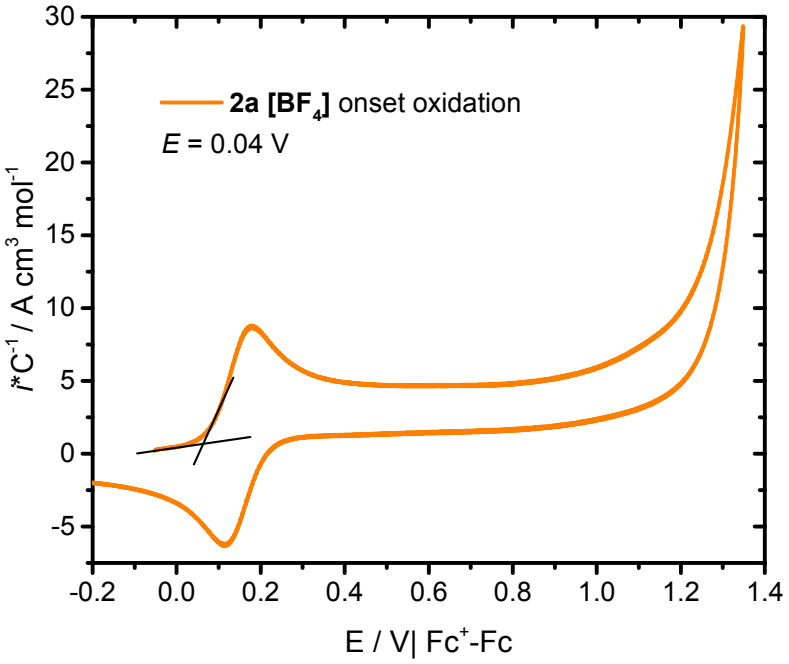

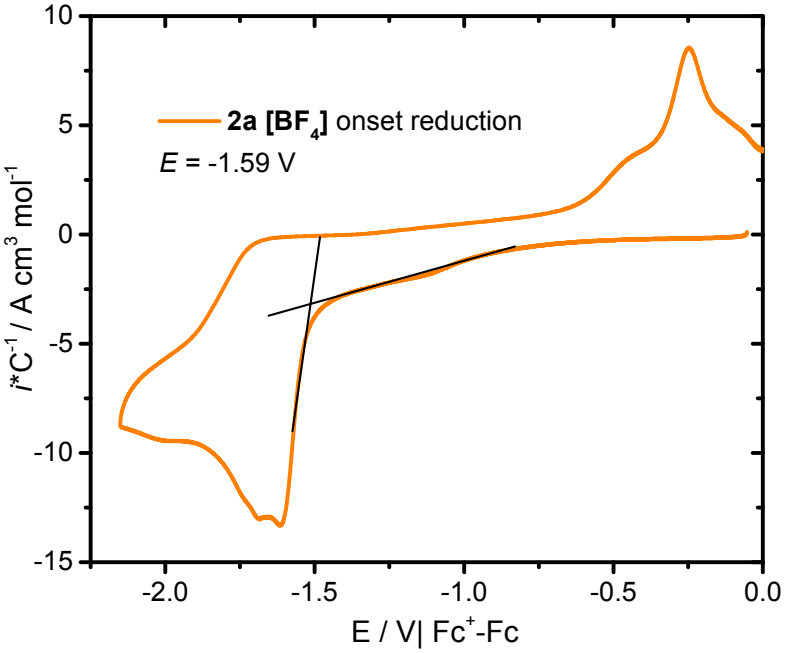

Figure S-40. Cyclic voltammograms to calculate the potential onset of oxidation and reduction for **2a[BF$_4$]**

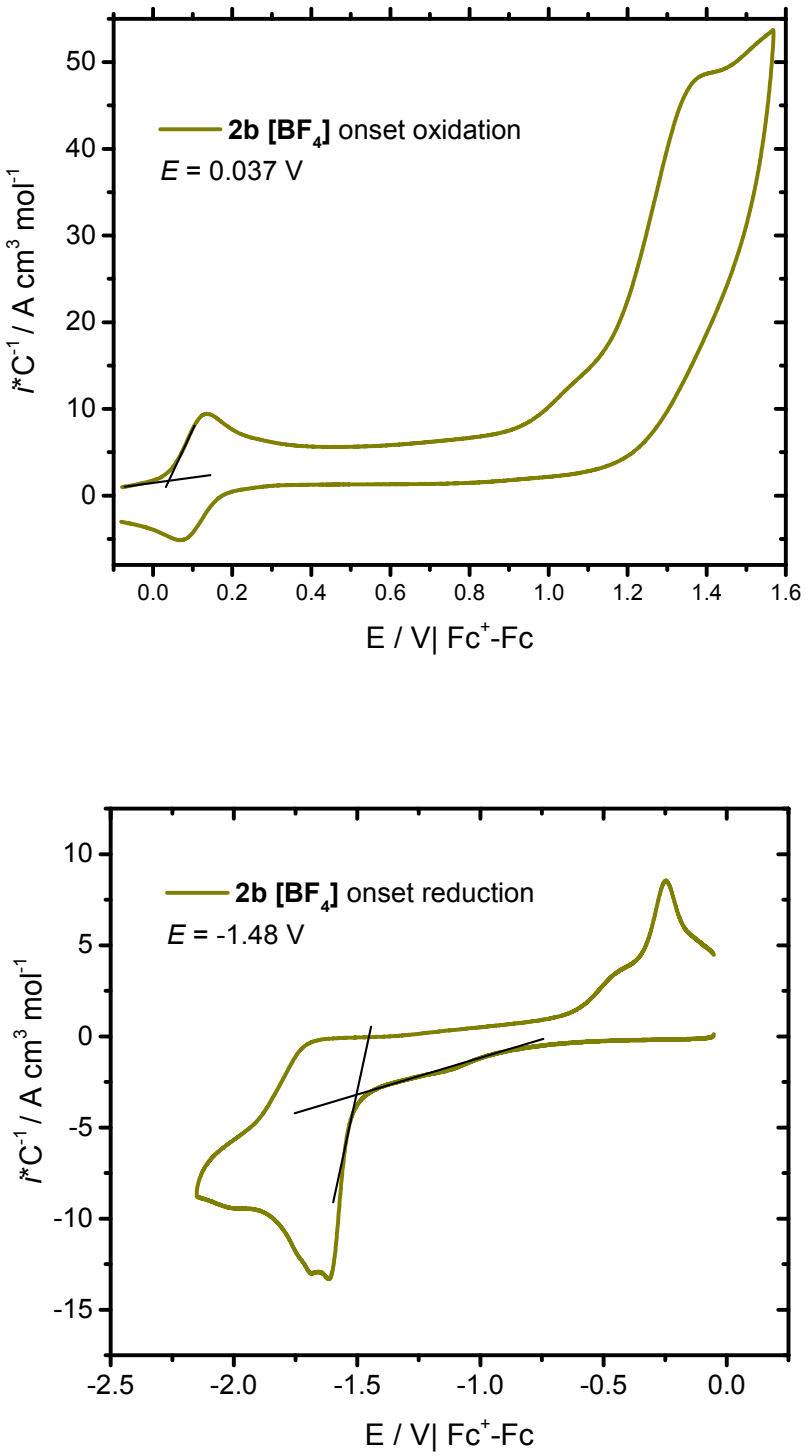

Figure S-41. Cyclic voltammograms to calculate the potential onset of oxidation and reduction for **2b**[BF_4].

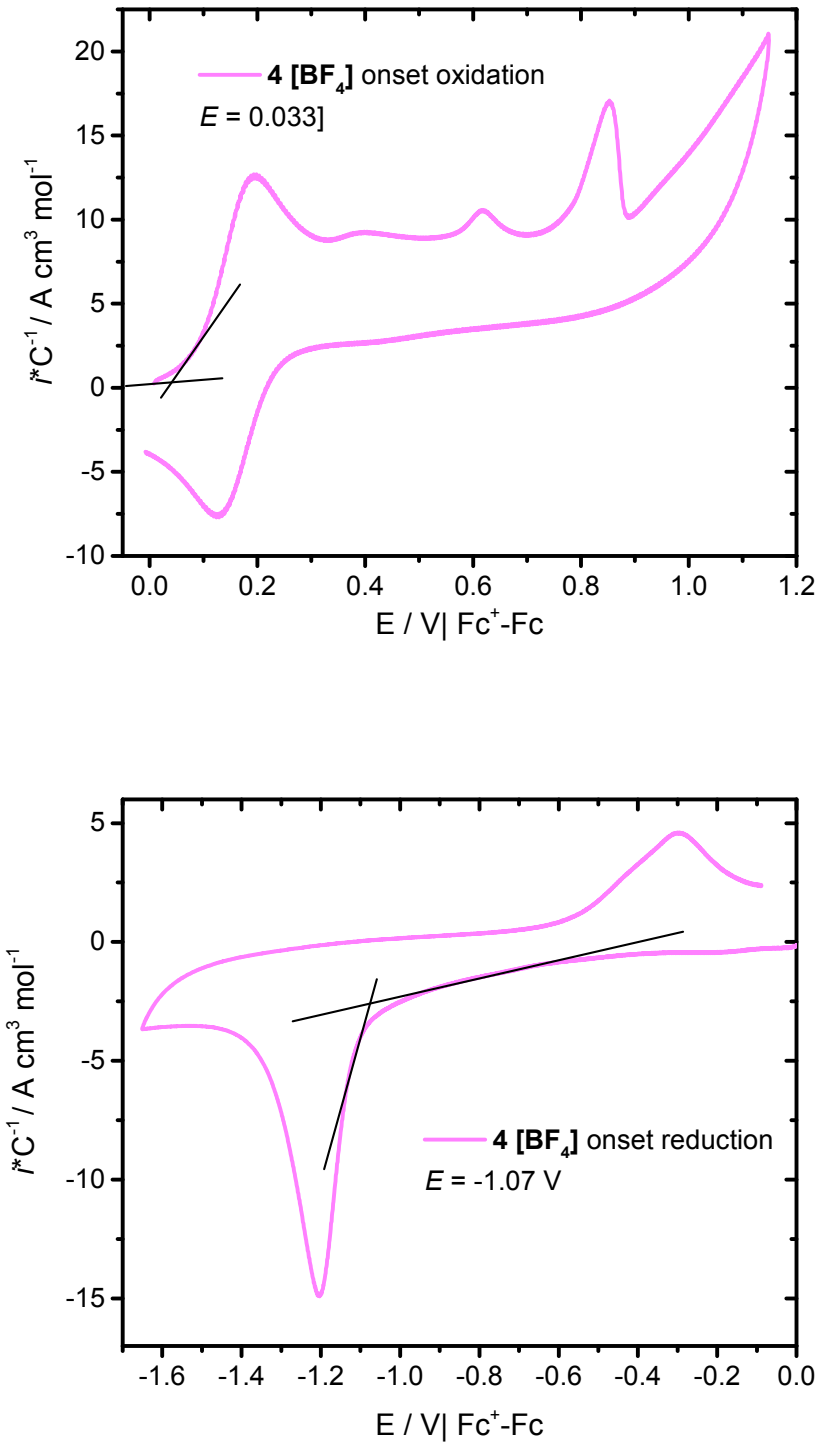

Figure S-42. Cyclic voltammograms to calculate the potential onset of oxidation and reduction for **4**[BF_4]

Computational Section: Optimized geometries

Compound 2a'

1 1

C	-1.25996300	1.72902700	0.26639200
C	-0.68413600	0.92946700	-0.78980300
C	-1.70659800	0.75380200	-1.79737600
C	-2.87043500	1.45896300	-1.37885300
C	-2.59546000	2.05782200	-0.10669700
H	-0.76850300	2.01871100	1.18733800
H	-1.59177100	0.18524700	-2.71260500
H	-3.81264100	1.50352900	-1.91151200
H	-3.29792800	2.62651000	0.49084800
Fe	-2.35170100	-0.00150400	0.00436300
C	-3.94533600	-1.31110100	0.12075600
C	-2.75295400	-2.02007900	-0.23160000
C	-3.72839200	-0.67937800	1.38631500
H	-4.84318500	-1.23655200	-0.48117200
C	-1.80003600	-1.82631200	0.81929100
H	-2.59021900	-2.57939200	-1.14510900
C	-2.40026300	-0.99740000	1.81833200
H	-4.43314900	-0.04386700	1.90912200
H	-0.78595800	-2.20793200	0.83629100
H	-1.92479500	-0.64944600	2.72750200
C	0.63412300	0.33806400	-0.86034500
H	0.77390500	-0.37203200	-1.67474900
C	1.67001400	0.64249100	-0.03616600
H	1.52301400	1.40231000	0.72454200
C	2.97400800	0.01226900	-0.11361300
N	4.04368200	0.61466800	0.50560800
C	3.20958500	-1.20560800	-0.77831400
C	5.28444000	0.06487400	0.47621600
C	4.47415700	-1.76517900	-0.82311900
H	2.37517000	-1.71715800	-1.24330800
H	6.05850900	0.61698000	0.99506400
H	4.63350300	-2.70551100	-1.34312500
C	5.53715800	-1.11870700	-0.18014000
H	6.54313900	-1.52306100	-0.17988300
C	3.87165500	1.89944300	1.21100200
H	3.44468700	2.63712700	0.52980600
H	4.84757700	2.24164100	1.54964700
H	3.21769500	1.76458600	2.07494500

Excited State 2: Singlet-A 2.0545 eV 603.47 nm f=0.0871 <S**2>=0.000

73 -> 77	-0.25597
73 -> 78	-0.10274
74 -> 75	0.51127
74 -> 76	0.12288
74 -> 77	0.10658
74 -> 78	-0.32788

Excited State 7: Singlet-A 3.1418 eV 394.63 nm f=0.7735 <S**2>=0.000
72 -> 75 0.65690
73 -> 77 0.15351
74 -> 76 0.14901

72 HOMO-2

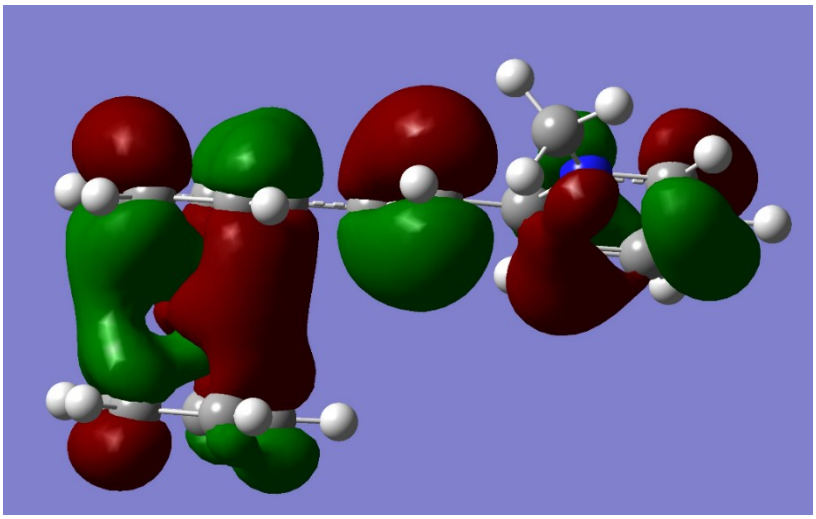

73 HOMO-1

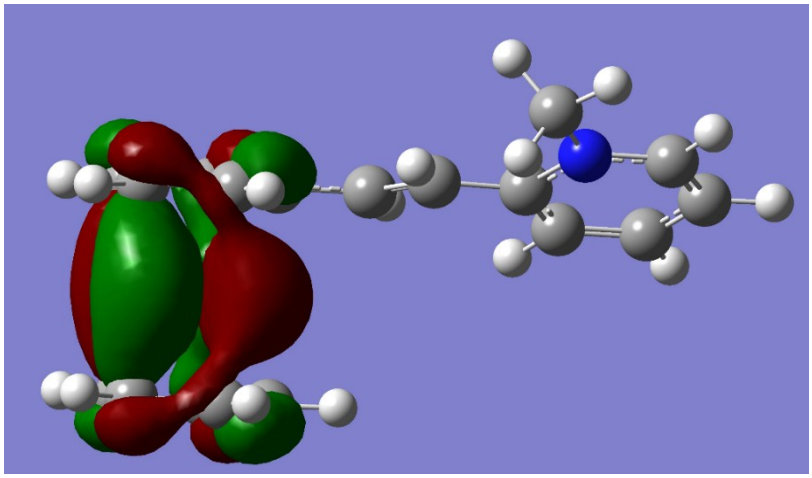

74 HOMO

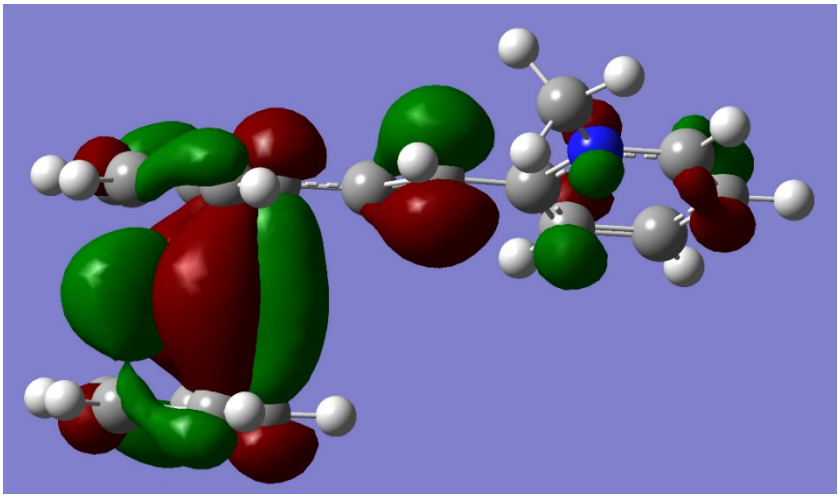

75 LUMO

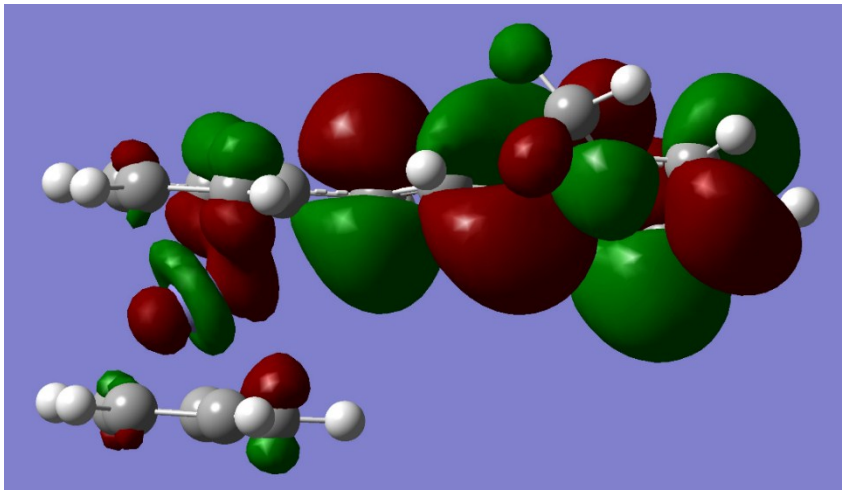

76 LUMO+1

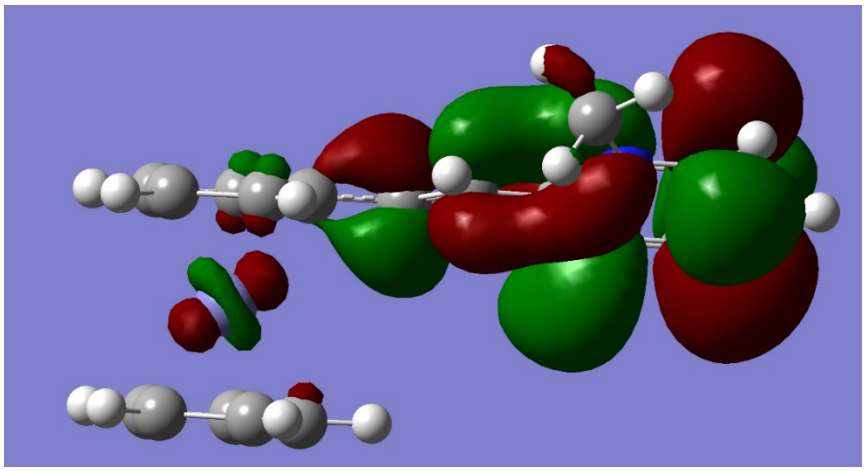

77 LUMO+2

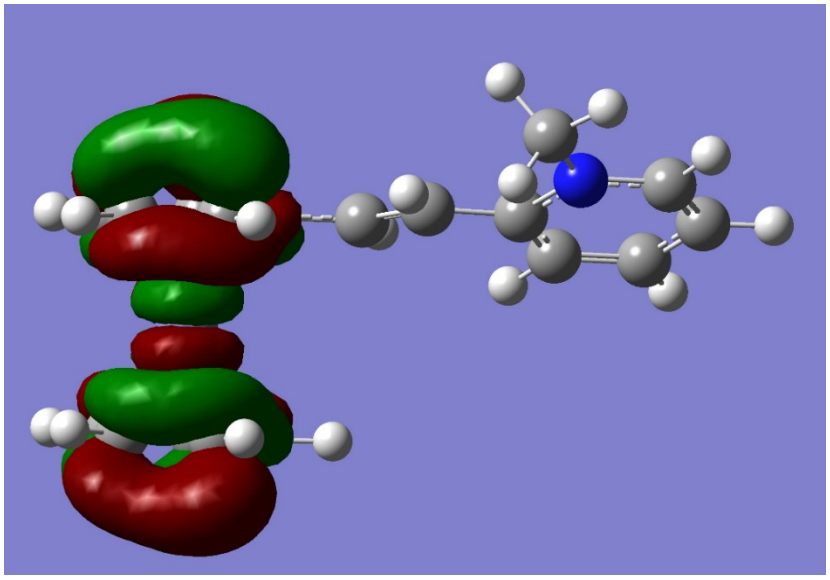

78 LUMO+3

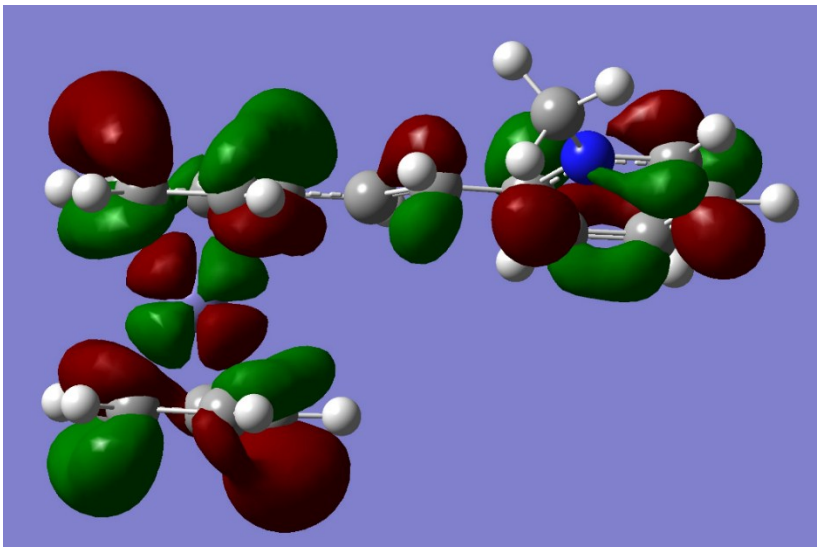

Compound 2b'

```
1 1
 C                  -0.94539300   -1.19862000   -0.38024900
 C                  -1.61736200   -1.58085700    0.84006500
 C                  -2.96435000   -1.91792200    0.51766400
 C                  -3.15152500   -1.73275100   -0.89023300
 C                  -1.92143400   -1.27677400   -1.44453600
 H                  -1.17814100   -1.60078400    1.82996700
 H                  -3.72708100   -2.22441500    1.22337400
 H                  -4.07805600   -1.87736000   -1.43269800
 H                  -1.73513600   -1.03035200   -2.48334600
```

Fe	-2.55458700	0.04912600	-0.00332500
C	-2.82831900	1.89470500	-0.89583900
C	-4.06128700	1.42087200	-0.34421000
C	-1.88093400	2.00096900	0.17190300
H	-2.63952800	2.11353400	-1.93999400
C	-3.87456300	1.23113400	1.06168900
H	-4.96657900	1.20702300	-0.89984000
C	-2.52456700	1.58770100	1.38102900
H	-0.84390000	2.29993800	0.07527100
H	-4.61377500	0.85019300	1.75632400
H	-2.06440700	1.52992400	2.36016700
C	0.42257900	-0.76211800	-0.56014100
H	0.64851600	-0.35754200	-1.54657800
C	1.40364900	-0.85181000	0.37469300
H	1.17409700	-1.28168900	1.34862600
C	2.77586100	-0.42313600	0.19235800
C	3.70435700	-0.60702800	1.24186000
C	3.27631200	0.17912400	-0.98823200
C	5.01907000	-0.21882400	1.10022100
H	3.39587100	-1.05948600	2.17913700
C	4.59765200	0.54465400	-1.07782300
H	2.64147500	0.36759700	-1.84683500
N	5.45862000	0.34717000	-0.04672100
H	5.75357200	-0.34764000	1.88650000
H	5.01723100	1.00567000	-1.96484500
C	6.86887900	0.74167000	-0.20233500
H	7.32553800	0.13951400	-0.99051200
H	7.38924800	0.57334400	0.73931000
H	6.91824100	1.79912800	-0.46783500

Excited State 2: Singlet-A 2.0052 eV 618.31 nm
f=0.1089 <S**2>=0.000

73 -> 78	-0.24415
74 -> 75	0.54490
74 -> 77	0.32885

Excited State 7: Singlet-A 3.0696 eV 403.92 nm
f=0.9265 <S**2>=0.000

72 -> 75	0.67027
73 -> 78	0.12908

72 HOMO-2

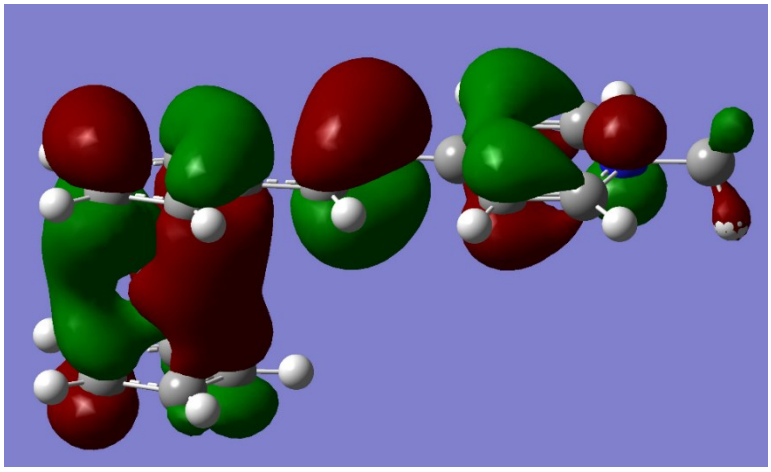

73 HOMO-1

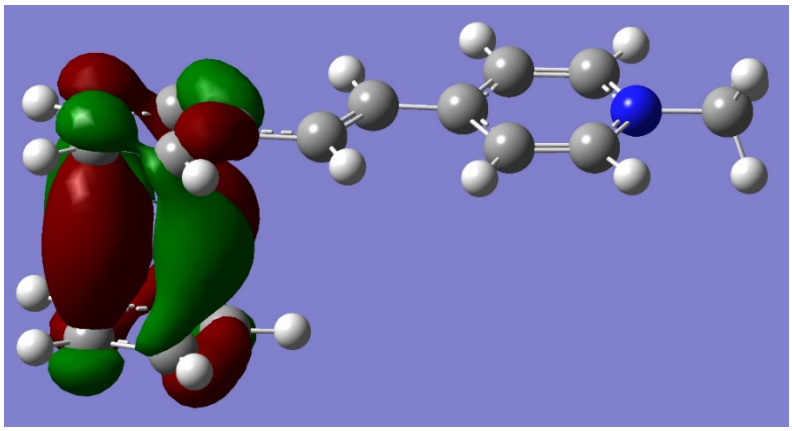

74 HOMO

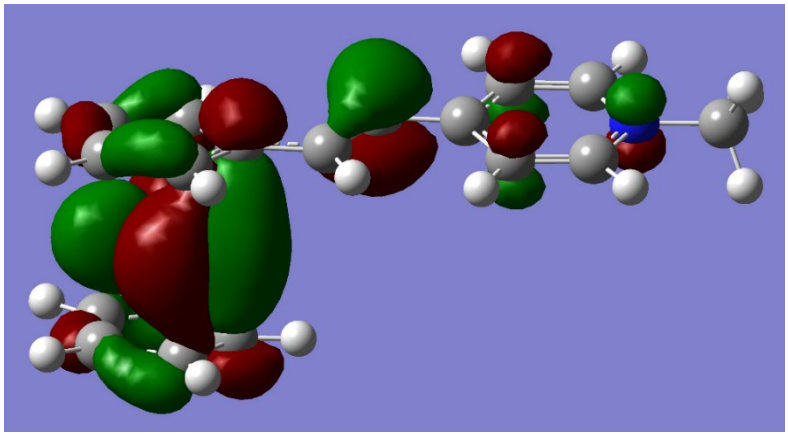

75 LUMO

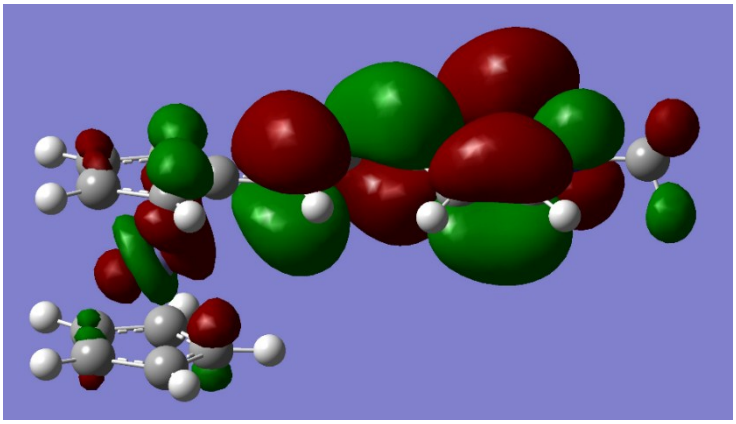

77 LUMO+2

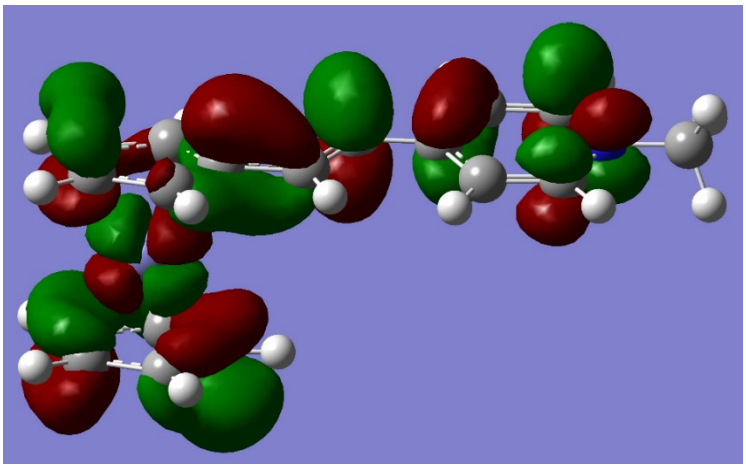

78 LUMO+3

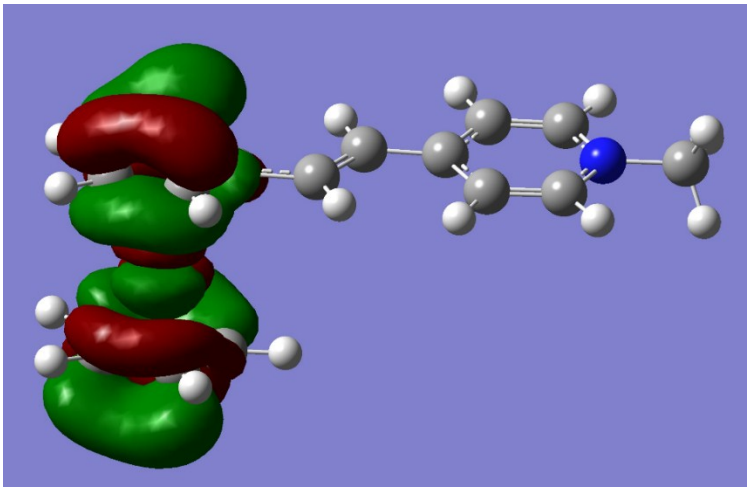

Compound 4′

```
1 1
 C                  1.65250800    0.54168200   -1.10710400
 C                  2.15152400    1.69127900   -0.38810900
 C                  3.49692400    1.91796000   -0.79740000
 C                  3.85739400    0.90992500   -1.74828300
 C                  2.73547900    0.05364200   -1.93270800
 H                  1.60230400    2.27543800    0.34013300
 H                  4.15080000    2.69393700   -0.41780500
 H                  4.82756300    0.79716000   -2.21673800
 H                  2.68468900   -0.81309400   -2.58101700
 Fe                 3.29392700    0.02786000    0.04807200
 C                  3.80939800   -1.91249100    0.55937400
 C                  4.93197900   -1.03926900    0.72226400
 C                  2.75896000   -1.44234200    1.41014100
 H                  3.75533800   -2.76266800   -0.10996200
 C                  4.57408800   -0.03019800    1.67131400
 H                  5.87277900   -1.10703600    0.18932000
 C                  3.22886000   -0.27834200    2.09577100
 H                  1.76798500   -1.87252100    1.49441700
 H                  5.19725900    0.79903200    1.98375500
 H                  2.65931900    0.32421900    2.79301400
 C                  0.35361200   -0.08620000   -1.01967300
 H                  0.27167100   -1.04060100   -1.53842100
 C                 -0.73489400    0.45127700   -0.40473800
 H                 -0.63196200    1.43668000    0.03893200
 C                 -2.03083200   -0.19176500   -0.32622700
 C                 -3.21878200    0.54490000    0.04147200
 C                 -2.19304600   -1.55781500   -0.59082300
 C                 -4.47983800   -0.13014400    0.10808500
 C                 -3.43627700   -2.15806500   -0.51967300
 H                 -1.34945000   -2.19151700   -0.83819200
 N                 -4.54641700   -1.48265700   -0.18725100
 H                 -3.56238700   -3.21507200   -0.72425500
 C                 -3.20183400    1.93403200    0.33454800
 H                 -2.27004200    2.48527500    0.28128500
 C                 -4.35217500    2.60990600    0.68403000
 H                 -4.31016300    3.67285700    0.90497900
 C                 -5.58109600    1.92439400    0.75288500
 H                 -6.48664200    2.45835800    1.02838100
 C                 -5.64979100    0.57488500    0.46763400
 H                 -6.60494600    0.06592800    0.52169500
 H                 -6.53761500   -1.74387100   -0.83233600
 C                 -5.83170700   -2.19659500   -0.13312000
 H                 -6.23561500   -2.15836100    0.88089500
 H                 -5.66078700   -3.23384100   -0.41514200


Excited State   2:      Singlet-A      1.8776 eV  660.34 nm  f=0.1696
<S**2>=0.000
      86 -> 91        -0.18215
      87 -> 88         0.60531
      87 -> 90         0.17331
```

```
      87 -> 92         0.20896

Excited State   6:      Singlet-A      2.7685 eV  447.85 nm  f=0.7363
<S**2>=0.000
      84 -> 88        -0.20464
      84 -> 92        -0.11356
      85 -> 88         0.62683
      86 -> 91        -0.16457
```

84 HOMO-3

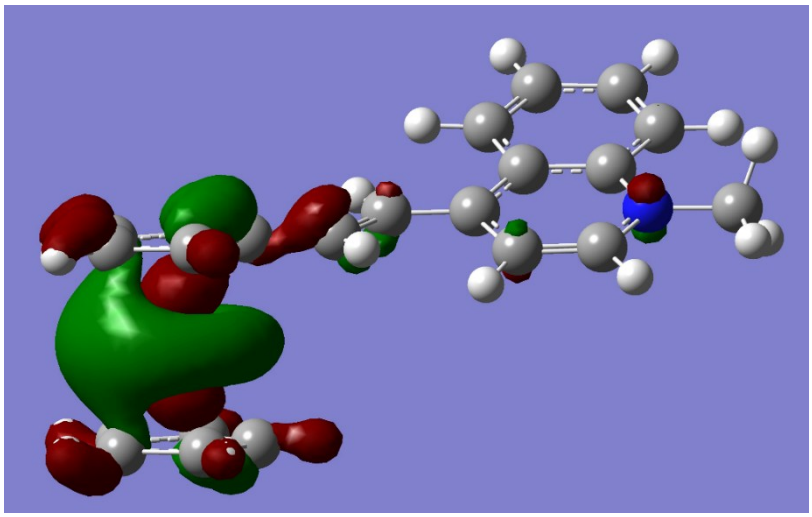

85 HOMO-2

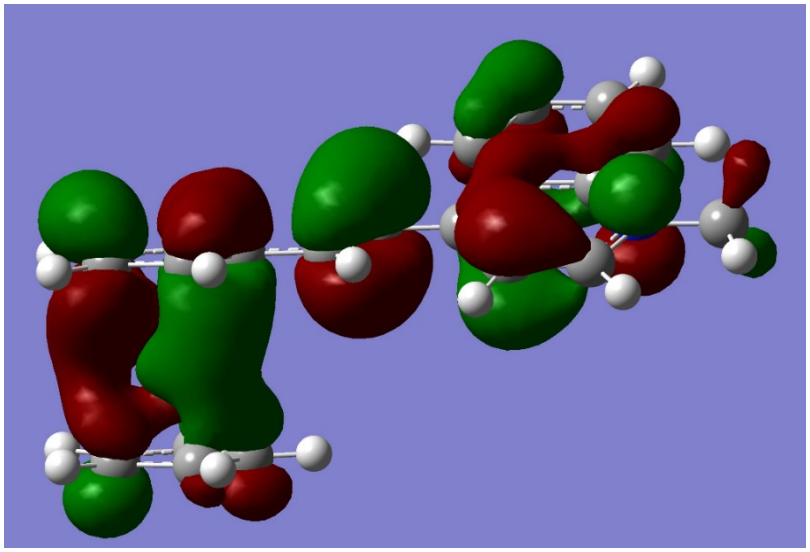

86 HOMO-1

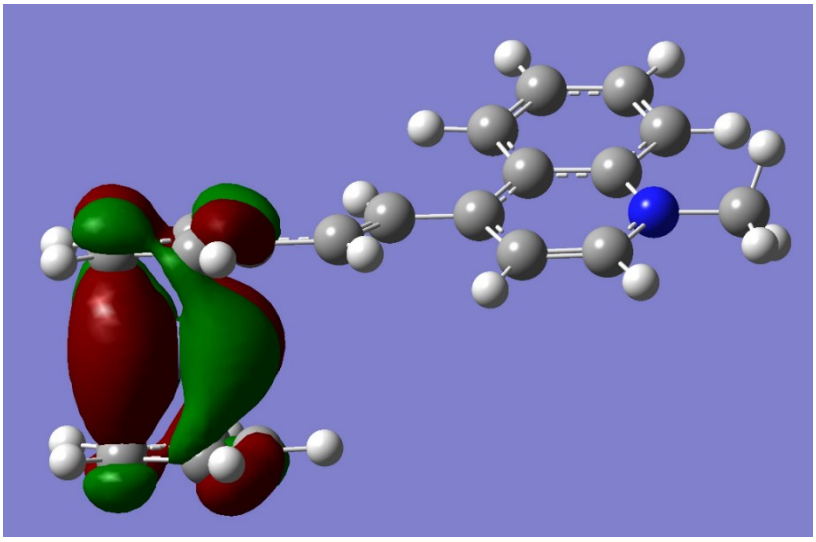

87 HOMO

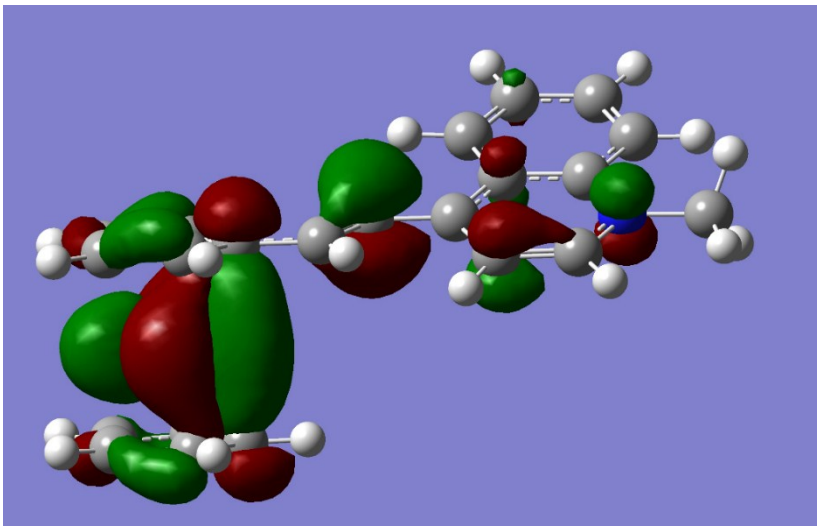

88 LUMO

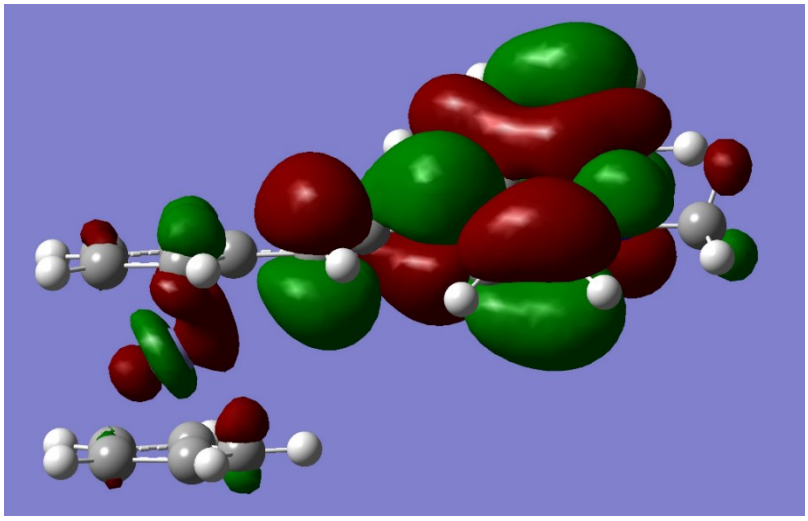

90 LUMO+2

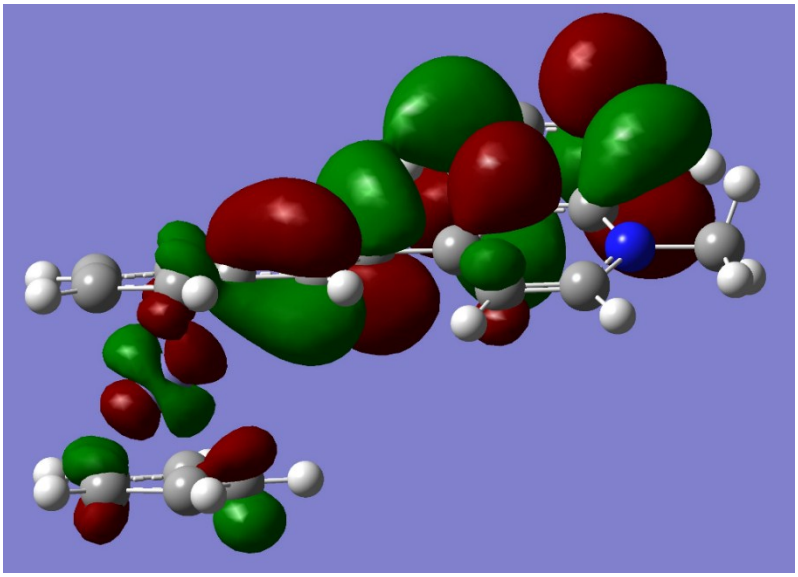

91 LUMO+3

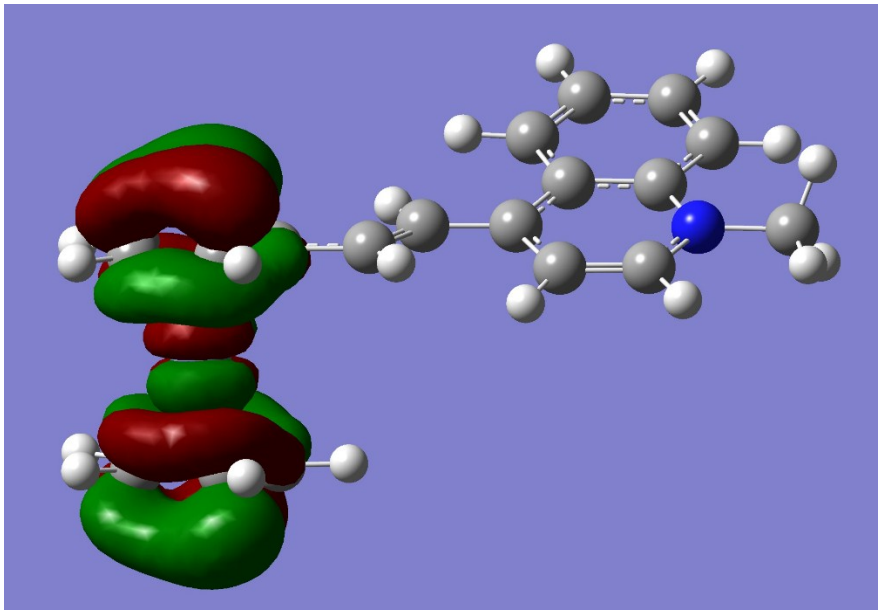

92 LUMO+4